Thermodynamics and kinetics of defect motion and annihilation in the self-assembly of lamellar diblock copolymers

Marcus Müller

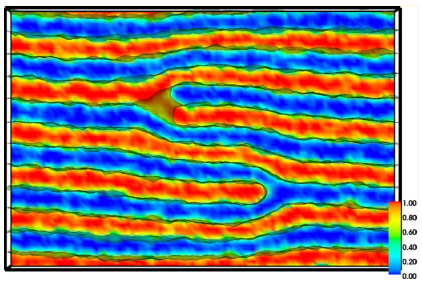

***outline*:**

- models and techniques
- defect motion – dislocation glide and climb
- defect annihilation mechanisms

collaborators:
Weihua Li, Ulrich Welling, Juan C. Orozco Rey,
Su-Mi Hur, Abelardo Ramirez-Hernandez,
Paul F. Nealey, Juan J. de Pablo

CoLiSA.MMP

GEORG-AUGUST-UNIVERSITÄT
GÖTTINGEN

Li. Müller, *Annual Rev. Chem. Biomol. Eng.* **6**, 187 (2015)
Li, Müller, *Prog. Polym. Sci.* **54–55**, 47 (2016)

UBC, Vancouver, August 1, 2017

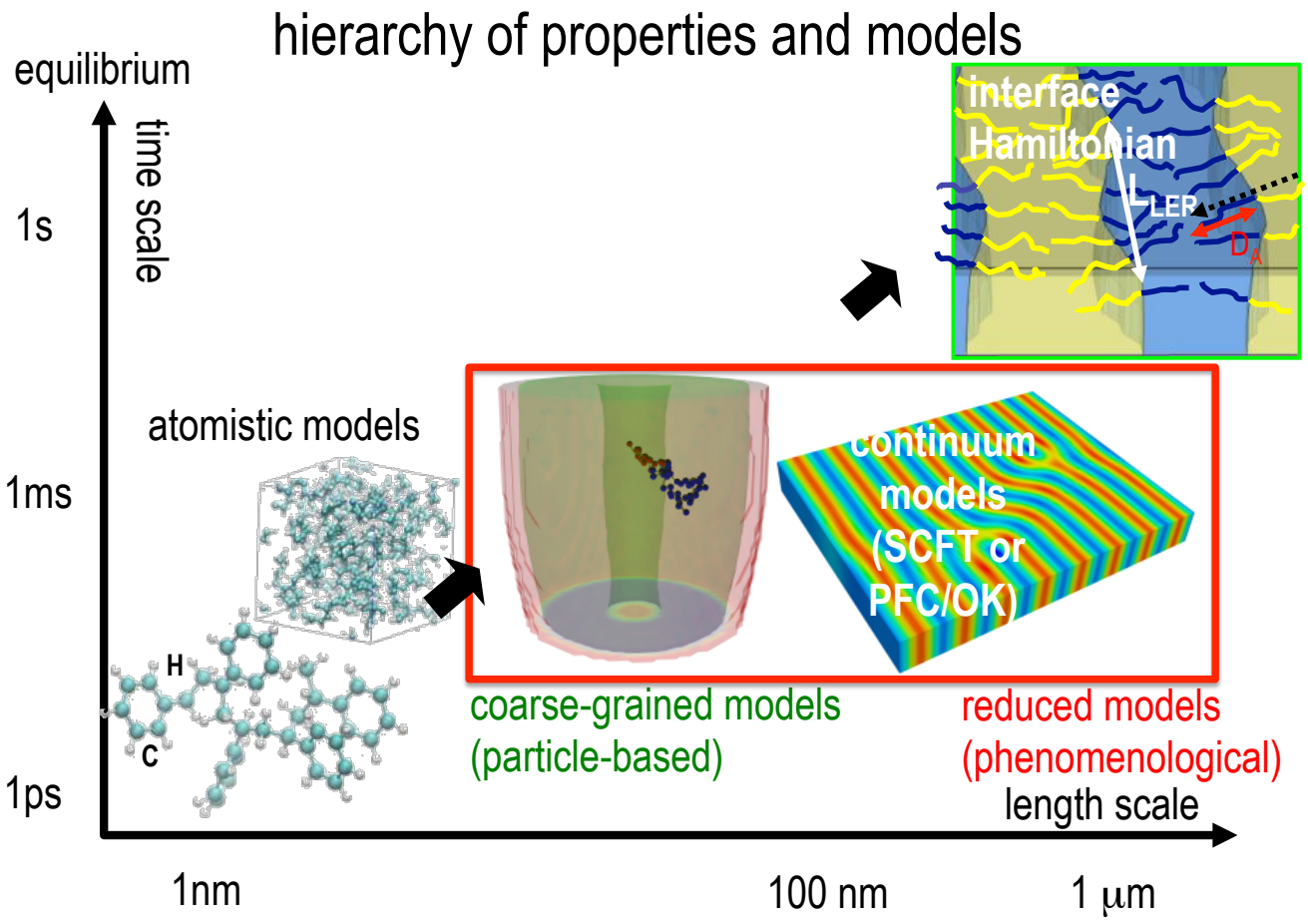
hierarchy of properties and models
equilibrium
time scale
1s
1ms
1ps
atomistic models
H
C
coarse-grained models
(particle-based)
continuum
models
(SCFT or
PFC/OK)
reduced models
(phenomenological)
length scale
1nm
100 nm
1 μm
Interface
Hamiltonian
LEP
D_A

top-down soft, coarse-grained models for copolymers

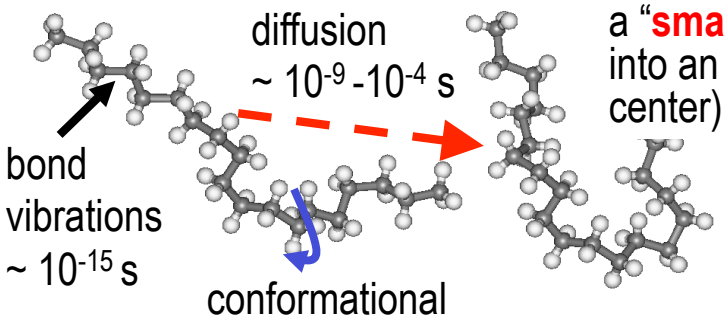

a "**small**" number of atoms is lumped into an effective segment (interaction center) MC,MD, DPD, LB, SCFT

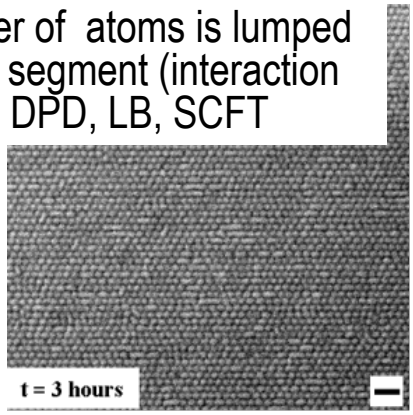

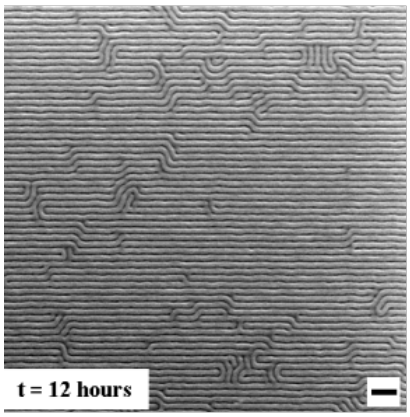

minimal coarse-grained model that captures only ***relevant interactions***: **connectivity, excl. volume, repulsion of unlike segments**

- incorporate essential interactions through a small number of effective parameters: chain extension, R_e, compressibility κN and Flory-Huggins parameter χN ➡ ***universality***
- elimination of degrees of freedom

➡ ***soft interactions***

Daoulas, Müller, JCP **125**, 184904 (2006)

top-down soft, coarse-grained models for copolymers

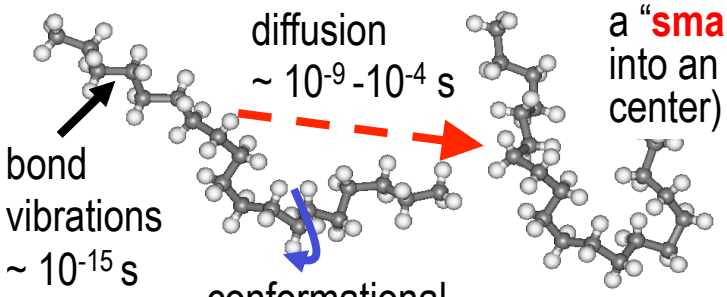

a "**small**" number of atoms is lumped into an effective segment (interaction center) MC,MD, DPD, LB, SCFT

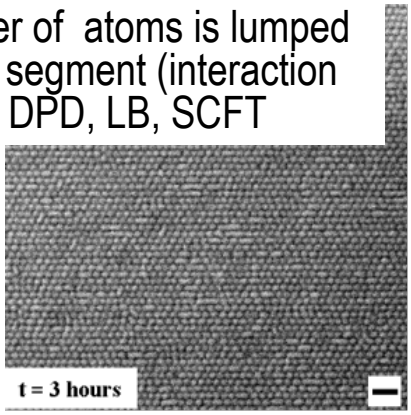

minimal coarse-grained model that captures only ***relevant interactions***: **connectivity, excl. volume, repulsion of unlike segments**

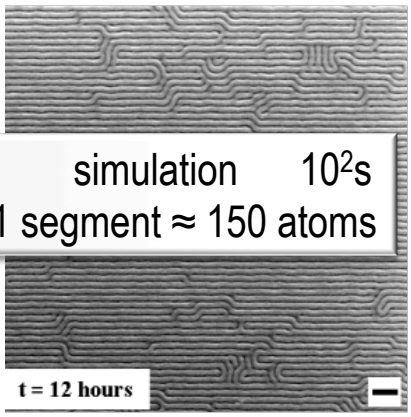

10^{-15}s minimal, soft, coarse-grained model 10^{-5}s simulation 10^{2}s

1 polymer ≈ 5000 (heavy) atoms ≈ 32 segments 1 segment ≈ 150 atoms

chain extension, R_e, compressibility κN and Flory-Huggins parameter χN ➡ ***universality***

- elimination of degrees of freedom

➡ ***soft interactions***

Daoulas, Müller, JCP **125**, 184904 (2006)

minimal, soft, coarse-grained models

bead-spring model with soft, pairwise interactions

$$\frac{\mathcal{H}_\mathrm{b}[\mathbf{r}_i(s)]}{k_BT} = \sum_{s=1}^{N-1} \frac{3(N-1)}{2{R_\mathrm{eo}}^2} \left[\mathbf{r}_i(s) - \mathbf{r}_i(s+1)\right]^2$$

$$\frac{\mathcal{H}_\mathrm{ord}[\hat{\phi}_A, \hat{\phi}_B]}{k_BT\sqrt{\bar{\mathcal{N}}}} = -\frac{\chi_\mathrm{o} N}{4} \int \frac{\mathrm{d}^3\mathbf{r}}{{R_\mathrm{eo}}^3} \left[\hat{\phi}_A(\mathbf{r}) - \hat{\phi}_B(\mathbf{r})\right]^2$$

$$\frac{\mathcal{H}_\mathrm{melt}[\hat{\phi}_A, \hat{\phi}_B]}{k_BT\sqrt{\bar{\mathcal{N}}}} = +\frac{\kappa_\mathrm{o} N}{2} \int \frac{\mathrm{d}^3\mathbf{r}}{{R_\mathrm{eo}}^3} \left[\hat{\phi}_A(\mathbf{r}) + \hat{\phi}_B(\mathbf{r}) - 1\right]^2$$

molecular architecture: Gaussian chain

with $\sqrt{\bar{\mathcal{N}}} \equiv \Phi_\mathrm{p} R_\mathrm{eo}^3$

effective interactions become weaker for large degree of coarse-graining

➡ no (strict) excluded volume, soft, effective segments can overlap, rather enforce low compressibility on length scale of interest, R_eo

$$\hat{\phi}_A(\mathbf{r}) = \frac{1}{\rho_\mathrm{o}} \sum_{i_A=1}^{nNf} \delta(\mathbf{r} - \mathbf{r}_{i_A})$$

$\hat{\phi}^2$-terms generate pairwise interactions

particle-based description for MC, BD, DPD, or SCMF simulations

Müller, Smith, J. Polym. Sci. B **43**, 934 (2005); Daoulas, Müller, JCP **125**, 184904 (2006); Detcheverry, Kang, Daoulas, Müller, Nealey, de Pablo, Macromolecules **41**, 4989 (2008); Pike, Detcheverry, Müller, de Pablo, JCP **131**, 084903 (2009); Detcheverry, Pike, Nealey, Müller, de Pablo, PRL **102**, 197801 (2009)

top-down soft, coarse-grained models for copolymers

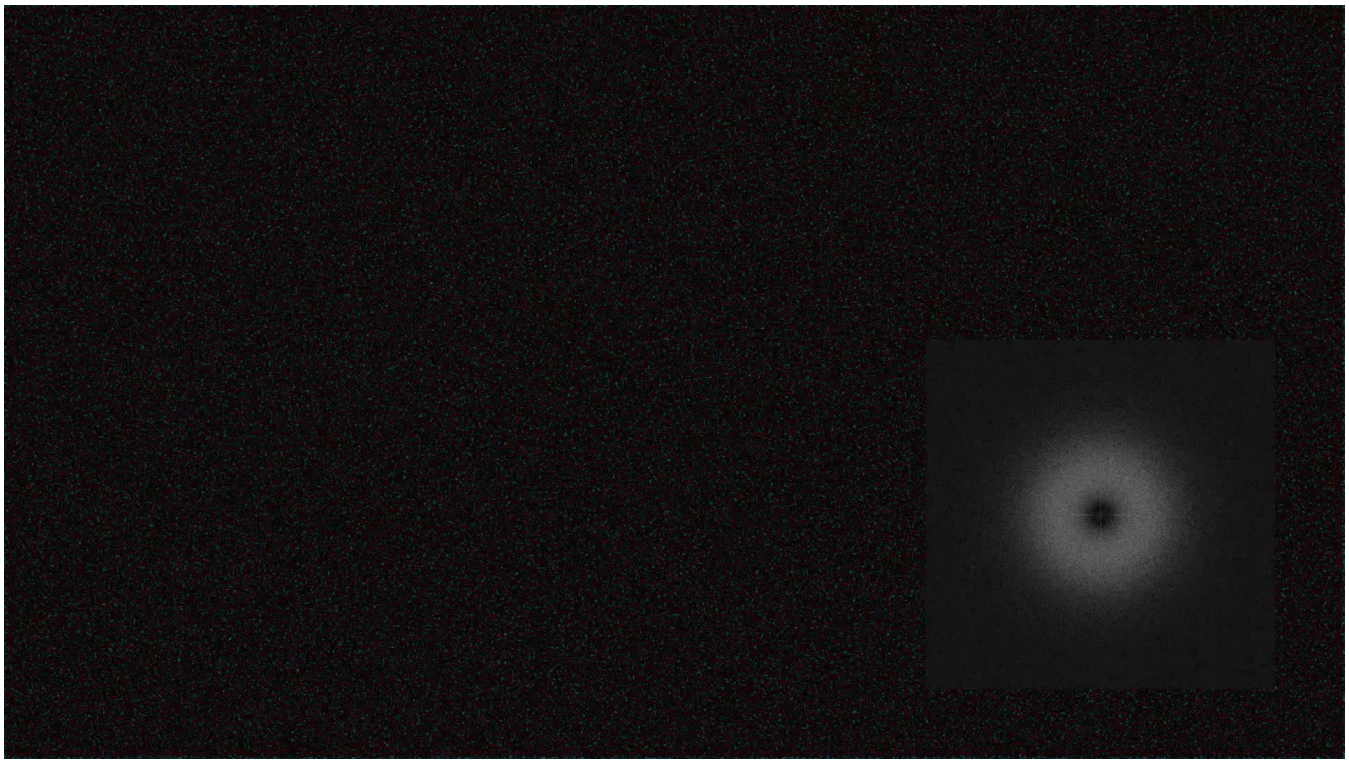

top-down soft, coarse-grained models for copolymers

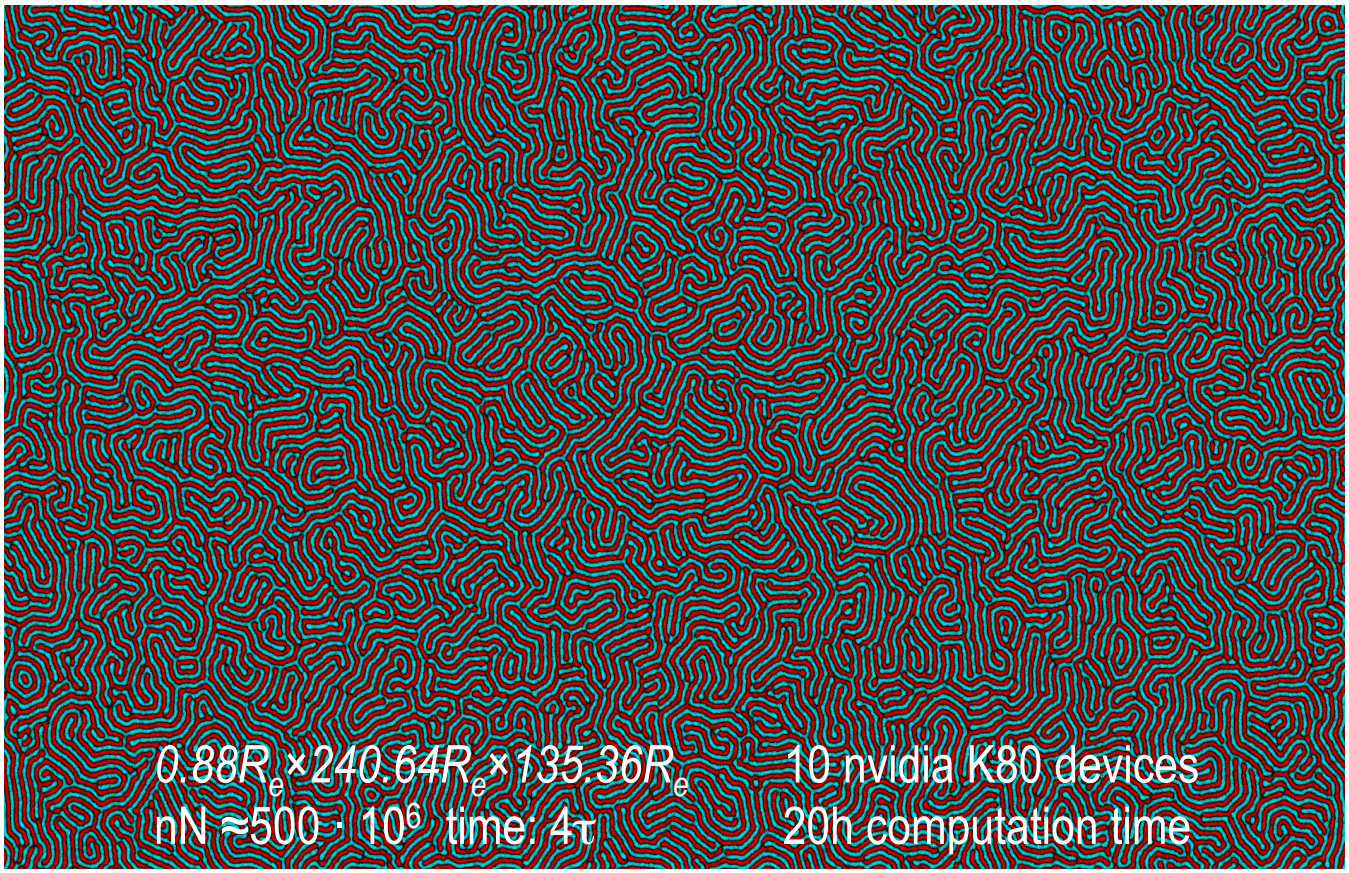

particle simulation and continuum description

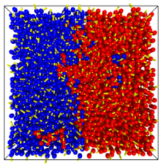

system: symmetric AB copolymer

degrees of freedom:

particle coordinates, $N(n_A + n_B)$
$\{\mathbf{r}_i(s)\}$

composition field (and density), ∞
$m(\mathbf{r}) = \phi_A(\mathbf{r}) - \phi_B(\mathbf{r})$
$\rho(\mathbf{r}) = \phi_A(\mathbf{r}) + \phi_B(\mathbf{r}) \approx \rho_o$

model definition:

intra- and intermolecular potentials
(here: soft, coarse-grained model, SCMF)

free-energy functional, $\mathcal{F}_{GL}[m(\mathbf{r})]$
(Ginzburg-Landau-de Gennes or Ohta-Kawasaki)

single-chain dynamics
(here: Rouse dynamics)

time-dependent GL theory
(model B according to Hohenberg & Halperin)

segmental friction, ζ

Onsager coefficient, $\Lambda(\mathbf{r} - \mathbf{r}')$

projection:

$$\hat{\phi}_A(\mathbf{r}) \text{“} = \text{”} \frac{1}{\rho_o} \sum_{i=1}^{n_A} \sum_{s=1}^{N} \delta\left(\mathbf{r} - \mathbf{r}_i(s)\right)$$

$$\frac{\mathcal{F}[m]}{k_B T} \equiv -\ln \int \mathcal{D}[\{\mathbf{r}_{i,s}\}]\, e^{-\frac{\mathcal{H}(\{\mathbf{r}_{i,s}\})}{k_B T}}\, \delta[m - (\hat{\phi}_A - \hat{\phi}_B)] \Rightarrow \mathcal{Z} \sim \int \mathcal{D}[m]\, e^{-\frac{\mathcal{F}[m]}{k_B T}}$$

$$\Lambda(\mathbf{r} - \mathbf{r}') = \left\langle \frac{\partial \hat{\phi}(\mathbf{r})}{\partial \mathbf{r}_i(s)} M_{\zeta,i,j}(s,t) \frac{\partial \hat{\phi}(\mathbf{r}')}{\partial \mathbf{r}_j(t)} \right\rangle$$

Kawasaki, Sekimoto, Physica **143A** , 349 (1987)

speed-up particle simulations by concurrent coupling

question: why are particle simulations slow?

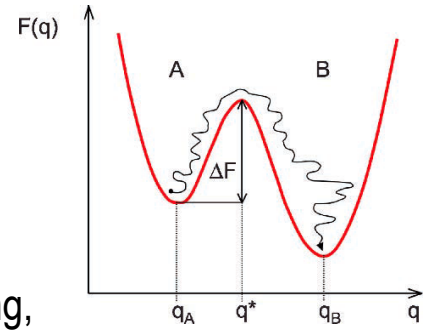

1) ***barrier problem (b)*:**

system has to overcome a **free-energy barrier**,

Kramer's theory $\tau \sim \exp(-\Delta F / k_B T)$

solutions: WL sampling, conf.T-WL, conf. flooding, metadynamics, transition-path sampling, forward flux sampling, …

Dellago, Bolhuis, Adv. Polym. Sci **221**, 167 (2008)

2) ***time-scale problem (a)*: "intrinsically slow processes"**

downhill in continuum free energy but **small Onsager coefficient** (response to TD force) and/or two **vastly different time scales** (stiff equations)

stiff interaction dictates time step, weak interaction drives slow time evolution

solutions:
- reversible multiple time step MD (RESPA) Tuckerman, Berne, Martyna, JCP **97**, 1990 (1992)
- SCMF simulation Müller, Smith J.Polym.Sci.B **43**, 934 (2005)
- **HMM** E, Engquist, Li, Ren, Vanden-Eijnden, Comm. Comp. Phys. **2**, 367 (2007)

free-energy functional from restraint simulations

idea: restrain the composition, $\hat{m} \equiv \hat{\phi}_A - \hat{\phi}_B$, of particle model to fluctuate around the order-parameter field, $m(\mathbf{r})$, of the continuum description (**field-theoretic umbrella sampling** for order-parameter field, $m(\mathbf{r})$)

$$\frac{\mathcal{H}_\mathrm{b}[\mathbf{r}_i(s)]}{k_BT} = \sum_{s=1}^{N-1} \frac{3(N-1)}{2{R_\mathrm{eo}}^2} \left[\mathbf{r}_i(s) - \mathbf{r}_i(s+1)\right]^2 \qquad \text{bead-spring model}$$

$$\frac{\mathcal{H}_\mathrm{nb}[\hat{\phi}_A,\hat{\phi}_B]}{k_BT\sqrt{\bar{\mathcal{N}}}} = \int \frac{\mathrm{d}^3\mathbf{r}}{R_\mathrm{eo}^3} \left(\frac{\kappa_\mathrm{o} N}{2} \left[\hat{\phi}_A + \hat{\phi}_B - 1\right]^2 - \frac{\chi_\mathrm{o} N}{4} \left[\hat{\phi}_A - \hat{\phi}_B\right]^2 \right) \qquad \text{soft, non-bonded}$$

$$\frac{\mathcal{H}_{\lambda N}}{k_BT\sqrt{\bar{\mathcal{N}}}} = \frac{\lambda N}{2} \int \frac{\mathrm{d}^3\mathbf{r}}{R_\mathrm{eo}^3} \left\{ \left[\hat{\phi}_A - \frac{1+m}{2}\right]^2 + \left[\hat{\phi}_B - \frac{1-m}{2}\right]^2 \right\} \qquad \text{restrain composition}$$

$\lambda N \gg \chi_\mathrm{o} N$ strong coupling between particle model and continuum description

$$\exp\left(-\frac{\mathcal{H}_{\lambda N}}{k_BT}\right) \overset{\lambda N\to\infty}{\to} \delta\left(m(\mathbf{r}) - \hat{\phi}_A + \hat{\phi}_B\right) \delta\left(\hat{\phi}_A + \hat{\phi}_B - 1\right)$$

$$\mu(\mathbf{r}) = \frac{\delta\mathcal{F}}{\delta m(\mathbf{r})} \overset{\lambda N\to\infty}{\approx} \frac{\delta\mathcal{F}_{\lambda N}}{\delta m(\mathbf{r})} = \left\langle \frac{\delta\mathcal{H}_{\lambda N}}{\delta m(\mathbf{r})} \right\rangle$$

$$\mu^* \equiv \frac{\mu R_\mathrm{eo}^3}{k_BT\sqrt{\bar{\mathcal{N}}}} \overset{\lambda N\to\infty}{\approx} \frac{\lambda N}{2}\left(m(\mathbf{r}) - \left\langle \hat{\phi}_A(\mathbf{r}) - \hat{\phi}_B(\mathbf{r}) \right\rangle\right) = \frac{\lambda N}{2}\left(m(\mathbf{r}) - \langle \hat{m}(\mathbf{r}) \rangle\right)$$

inspired by Maragliano, Vanden-Eijnden, *Chem. Phys. Lett.* **426**, 168 (2006)
Müller, Daoulas, *Phys. Rev. Lett.* **107**, 227801 (2011)

continuum models

Self-Consistent-Field Theory (SCFT) [classical DFT for copolymers/MFA]

Leibler's RPA: systematic expansion in order parameter $\Psi = \phi_A - f$

$$\frac{\mathscr{F}[\Psi]}{k_B T} = +\frac{1}{2!}\int \frac{d\mathbf{q}}{(2\pi)^3}\,\gamma_2(\mathbf{q})\Psi_{\mathbf{q}}\Psi_{-\mathbf{q}} +\frac{1}{3!}\int \frac{d\mathbf{q}_1\,d\mathbf{q}_2}{(2\pi)^6}\,\gamma_3(\mathbf{q}_1,\mathbf{q}_2)\Psi_{\mathbf{q}_1}\Psi_{\mathbf{q}_2}\Psi_{-\mathbf{q}_1-\mathbf{q}_2}$$

0 for symmetric copolymers, f=1/2

$$+\frac{1}{4!}\int \frac{d\mathbf{q}_1\,d\mathbf{q}_2\,d\mathbf{q}_3}{(2\pi)^9}\,\gamma_4(\mathbf{q}_1,\mathbf{q}_2,\mathbf{q}_3)\Psi_{\mathbf{q}_1}\Psi_{\mathbf{q}_2}\Psi_{\mathbf{q}_3}\Psi_{-\mathbf{q}_1-\mathbf{q}_2-\mathbf{q}_3}$$

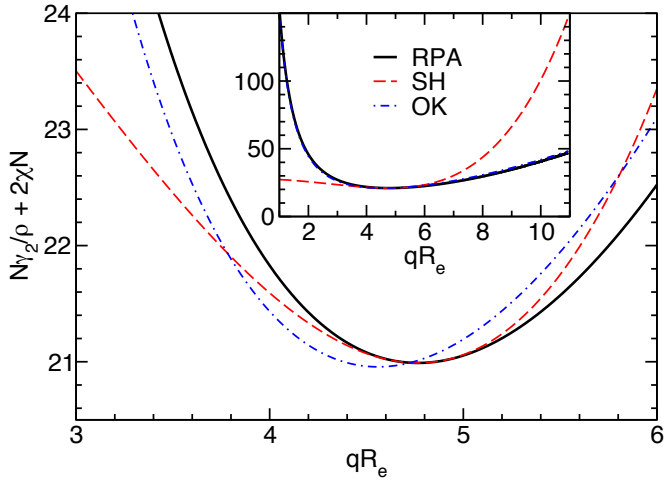

PFC / Swift-Hohenberg model

$$\frac{N}{\rho}\gamma_{2-\mathrm{SH}}(q) = \tau_0 + \varepsilon_0\left[(q^* R_e)^2 - (qR_e)^2\right]^2$$

Ohta-Kawasaki model

$$\frac{N}{\rho}\gamma_{2-\mathrm{OK}}(q) = \frac{(qR_e)^2}{3} + 7.1 - 2\chi N + \frac{144}{(qR_e)^2}$$

continuum models

PFC / Swift-Hohenberg model

$$\mathcal{F}_{\mathrm{SH}}[m] = \int \mathrm{d}\mathbf{x} \left(\frac{1}{2} m \left\{ -\tilde{\epsilon} + [1 + \triangle]^2 \right\} m + \frac{1}{4} m^4 \right)$$

Ohta-Kawasaki model

$$\mathcal{F}_{\mathrm{OK}}[m] = \int \mathrm{d}\mathbf{x} \left(\frac{1}{2} m \left\{ -\triangle - 1 + \tilde{\alpha} \int \mathrm{d}\mathbf{x}' \, G(\mathbf{x}, \mathbf{x}') \right\} m + \frac{1}{4} m^4 \right)$$

conserved dynamics (model B)

$$\frac{\partial m}{\partial t} = -\nabla \mathbf{j} = \Lambda \triangle \frac{\delta \mathcal{F}}{\delta m(\mathbf{x})}$$

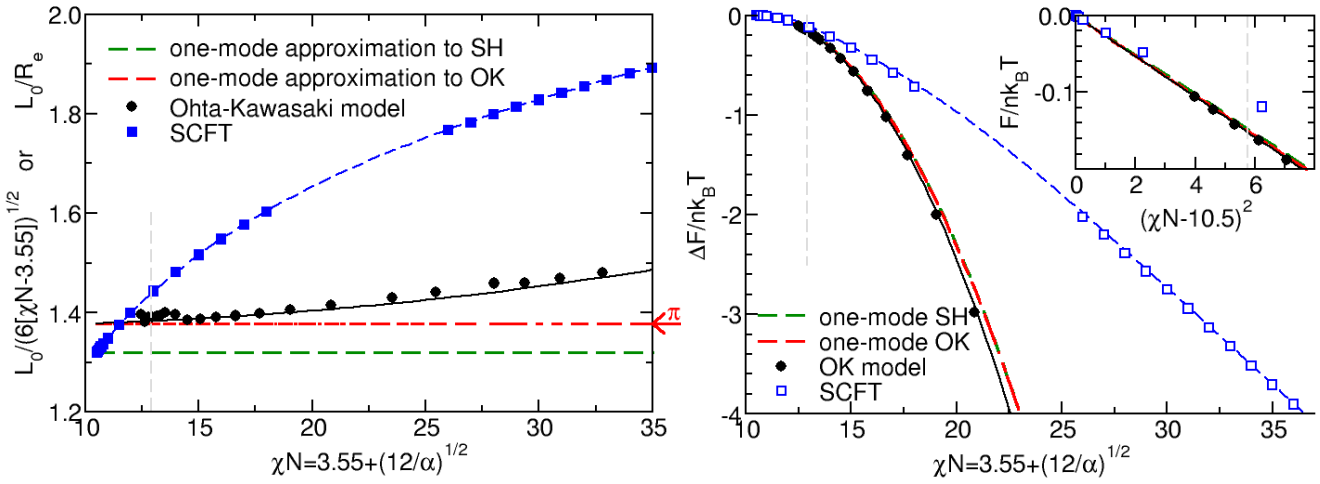

continuum models

PFC / Swift-Hohenberg model	*versus*	Ohta-Kawasaki model
+ no long-range part in free-energy		- long-range (Coulomb) contribution to free energy [but model B dynamics with local Onsager coefficient is not long-ranged]
- higher-order spatial derivative		
- predicts macrophase separation between spatially modulated phases (and disordered structures) for asymmetric compositions		+ qualitative agreement with phase diagram
- tight dislocation pairs are unstable in relevant parameter range		+ tight dislocation pairs exhibit transition from unstable to meta-stable at intermediate segregation

copolymer lithography:
directed assembly of copolymers into nanostructures

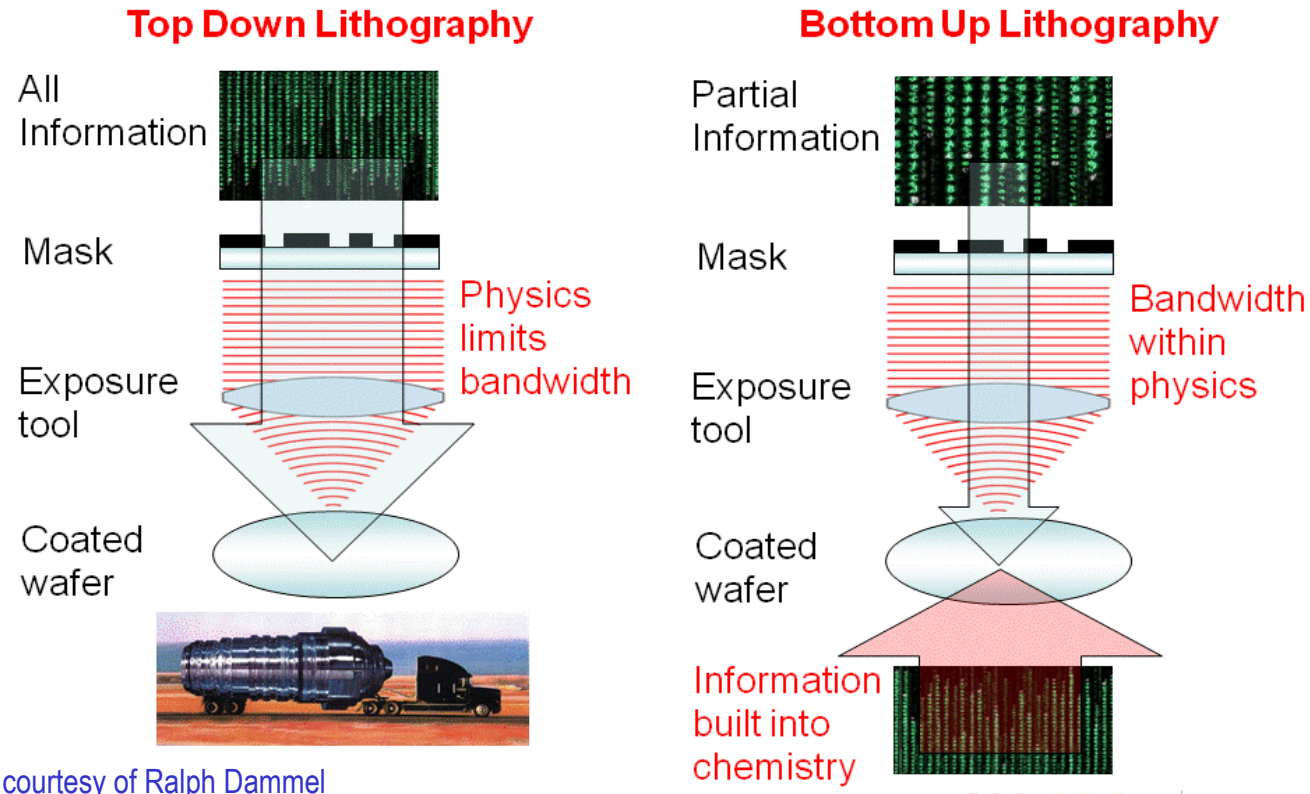

courtesy of Ralph Dammel
http://www.nikonprecision.com/ereview/spring_2013/images/featured-4L.gif

defect free energy for lamellar pattern replication

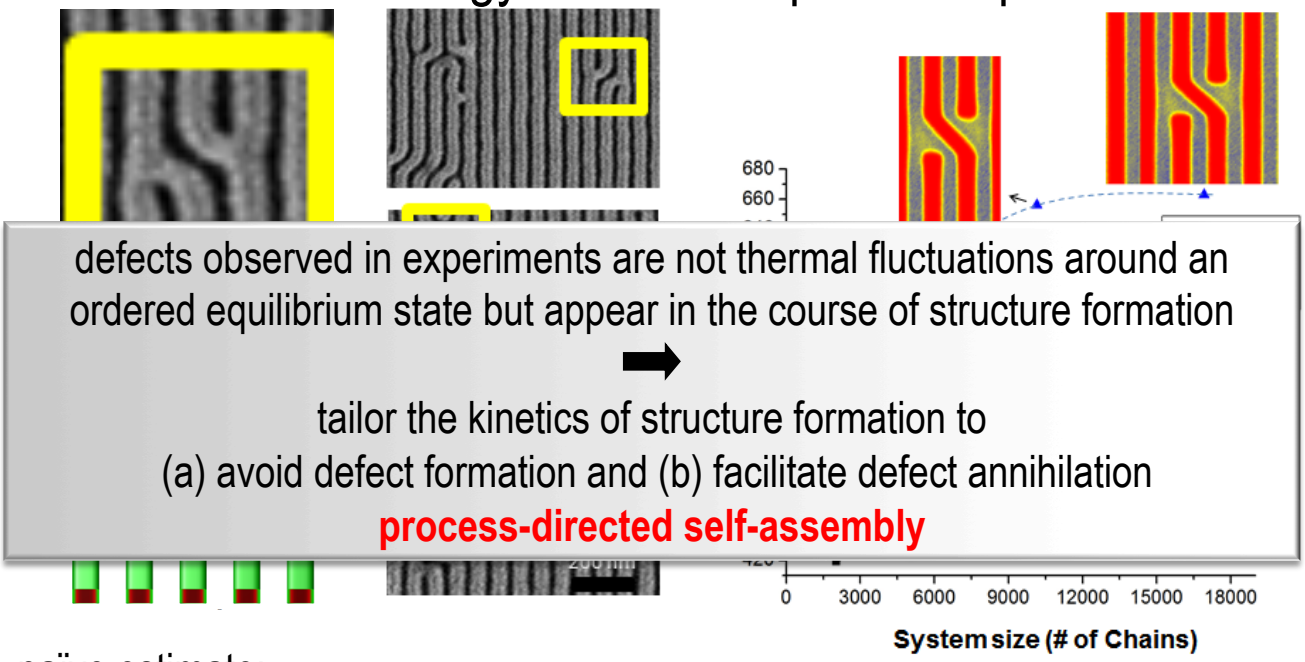

defects observed in experiments are not thermal fluctuations around an ordered equilibrium state but appear in the course of structure formation

➡

tailor the kinetics of structure formation to
(a) avoid defect formation and (b) facilitate defect annihilation

process-directed self-assembly

naïve estimate:

$$\Delta F = \gamma A \approx \frac{\sqrt{N} k_B T}{{R_{eo}}^2} \times 2 L_s D_o$$

$$\approx 128 k_B T \times 3.6 = 460 k_B T$$

➡ extremely small defect density **in equilibrium**

$\Delta F_d = 30 k_B T$ ➔ $\sigma_d \sim 0.001/cm^2$

Nagpal, Müller, Nealey, de Pablo, *ACS Macro Letters* **1**, 418 (2012)

ordering kinetics: SCMF simulations

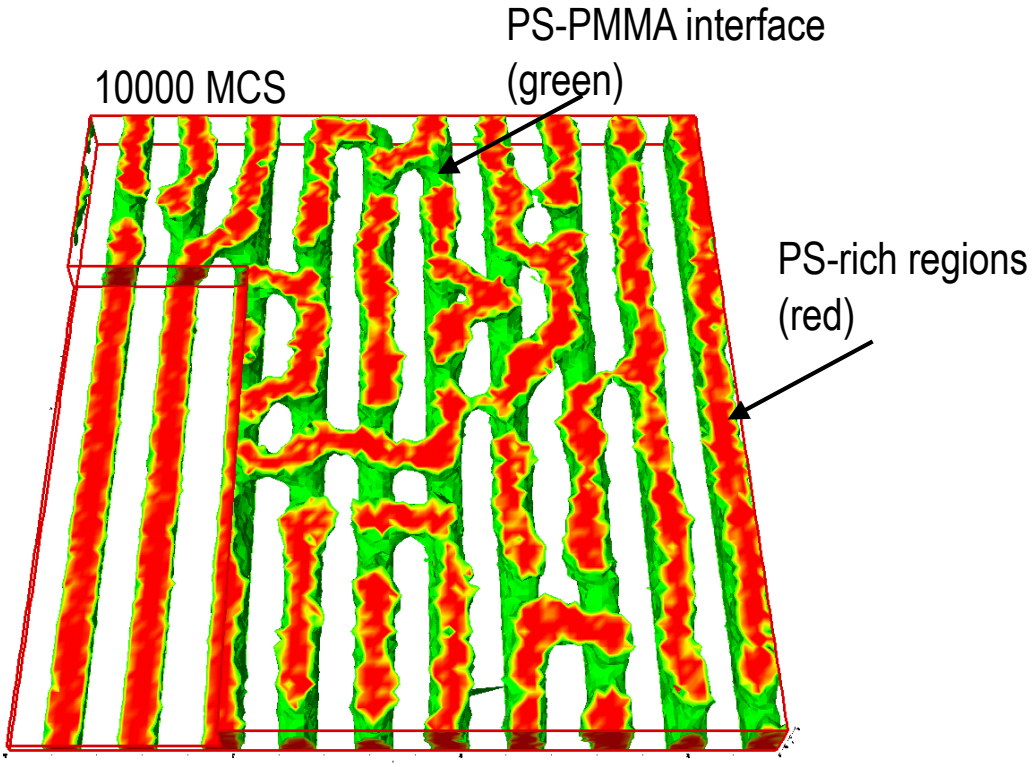

Edwards, Stokovich, Müller, Solak, de Pablo, Nealey, *J. Polym.* Sci B **43**, 3444 (2005)

ordering kinetics: SCMF simulations

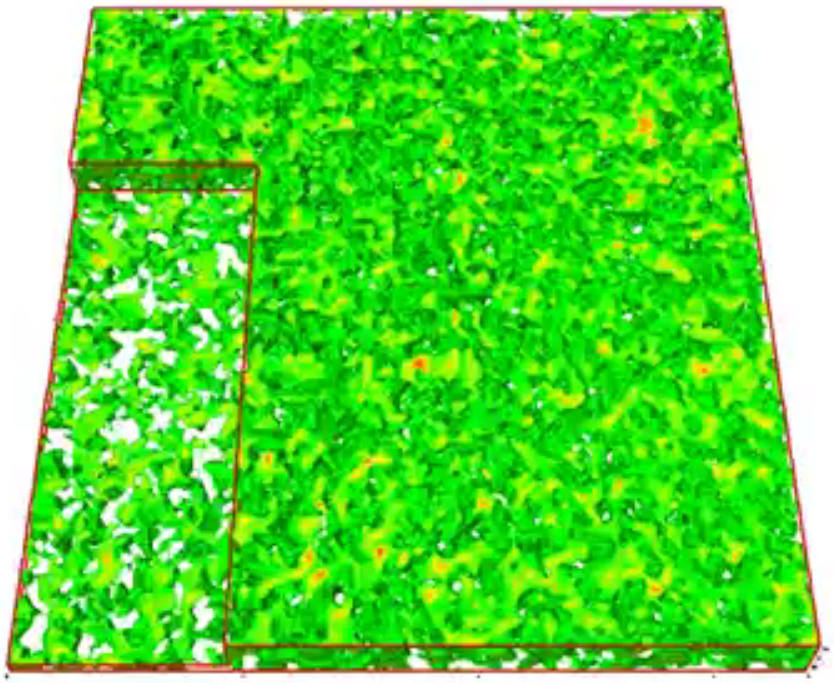

ordering kinetics: SCMF simulations

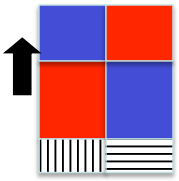

1) surface pattern directs spinodal self-assembly into a checkerboard pattern (bottom registered, top anti-registered)

2) interface between registered and anti-registered grain shifts upwards and the anti-registered grain become thinner and breaks up (dots)

➡ perfect order is established by perpendicular interface movement (instead of lateral defect motion and annihilation)

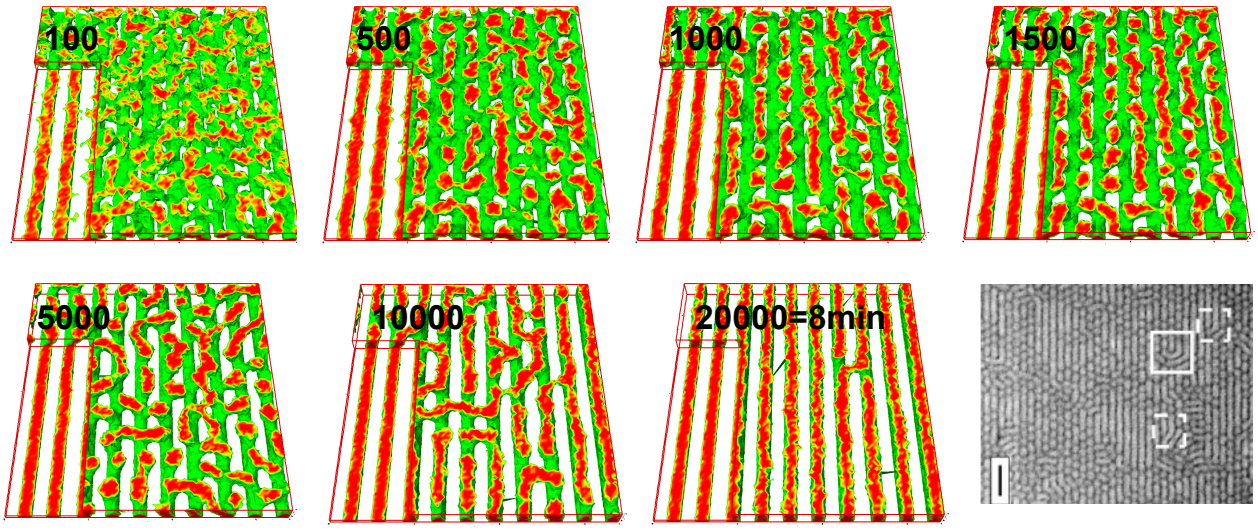

ordering kinetics: SCMF simulations

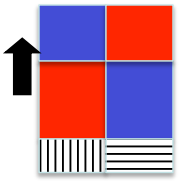

1) surface pattern directs spinodal self-assembly into a checkerboard pattern (bottom registered, top anti-registered)

2) interface between registered and anti-registered grain shifts upwards and the anti-registered grain become thinner and breaks up (dots)

➡ perfect order is established by perpendicular interface movement (instead of lateral defect motion and annihilation)

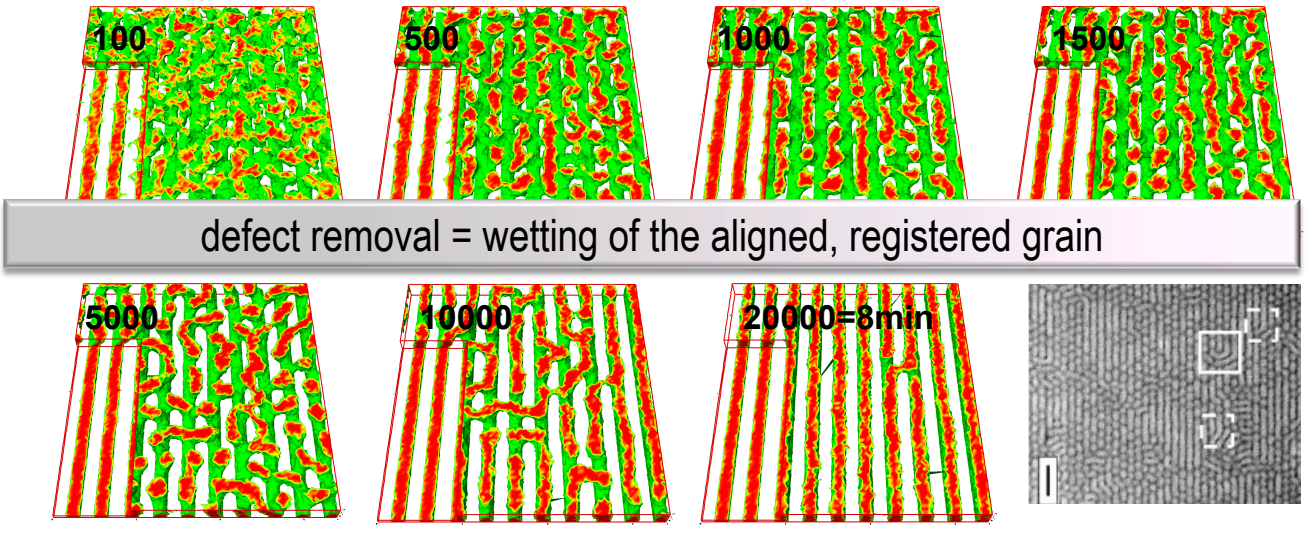

process-directed self-assembly

SCMF simulation of DSA under non-optimal conditions:
weak surface interaction $\Lambda N = 0.1$ and period mismatch $L_S = 1.8\bar{3}R_{\mathrm{eo}}$

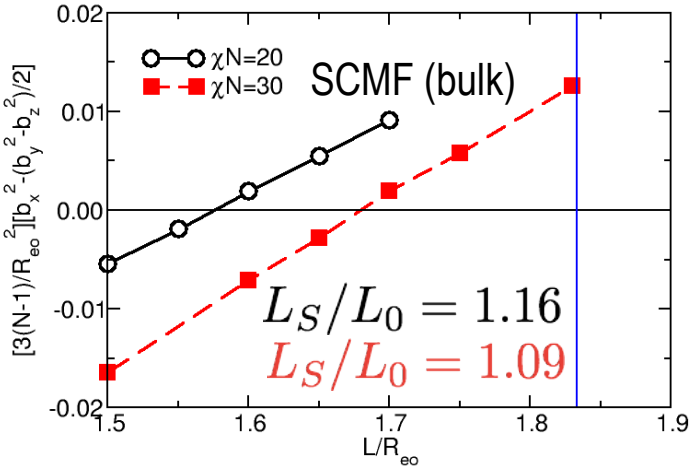

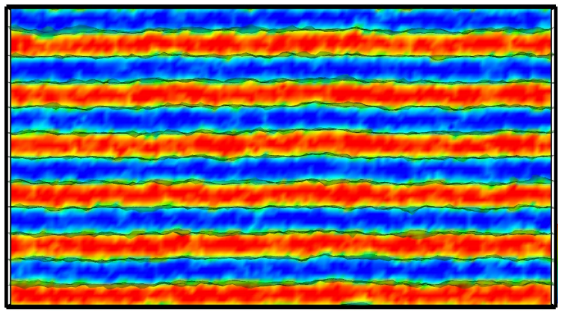

high incompatibility: $L_0 \approx 1.68R_{\mathrm{eo}}$ $@\chi N = 30$ **small mismatch**

low incompatibility: $L_0 \approx 1.58R_{\mathrm{eo}}$ $@\chi N = 20$ **large mismatch**

process-directed self-assembly

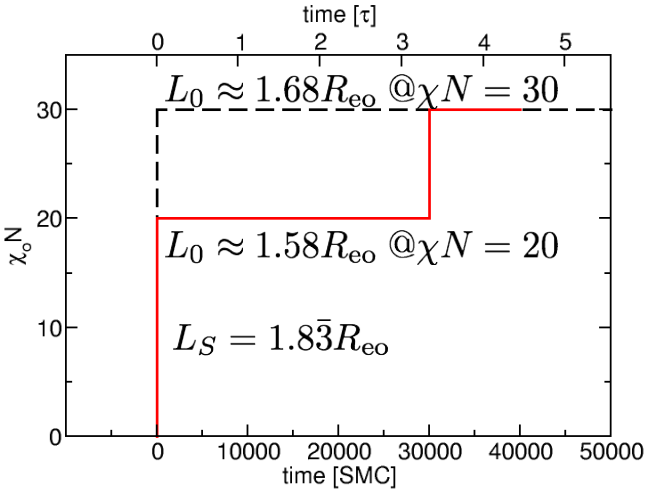

process-directed self-assembly:

1) one-step quench:

$$\chi_0 N = 0 \rightarrow 30$$

2) two-step quench:

$$\chi_0 N = 0 \rightarrow 20 \rightarrow 30$$

process-directed self-assembly

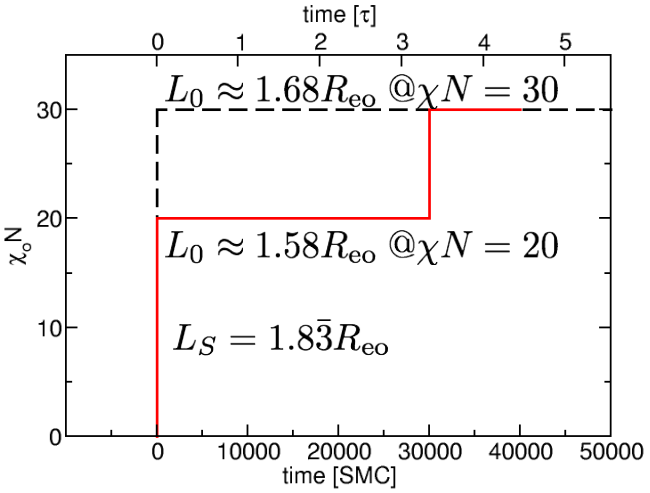

process-directed self-assembly:

1) one-step quench:

$$\chi_0 N = 0 \rightarrow 30$$

2) two-step quench:

$$\chi_0 N = 0 \rightarrow 20 \rightarrow 30$$

➡ observation: two-step quench results in pattern replication although …

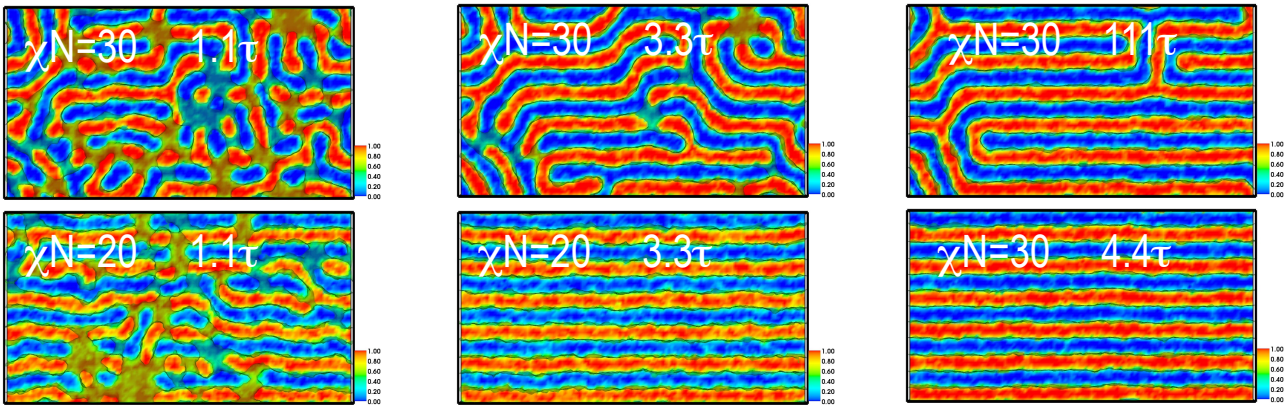

process-directed self-assembly

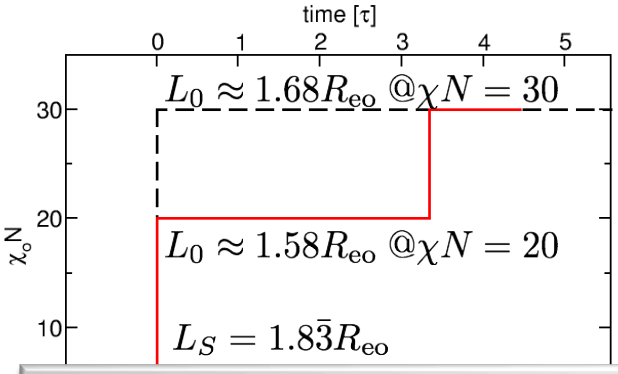

process-directed self-assembly:

1) one-step quench:

$$\chi_0 N = 0 \rightarrow 30$$

2) two-step quench:

$$\chi_0 N = 0 \rightarrow 20 \rightarrow 30$$

why does the two-step process that gives rise to a “worse” match between the guiding pattern and the equilibrium structure yields defect-free self-assembly?

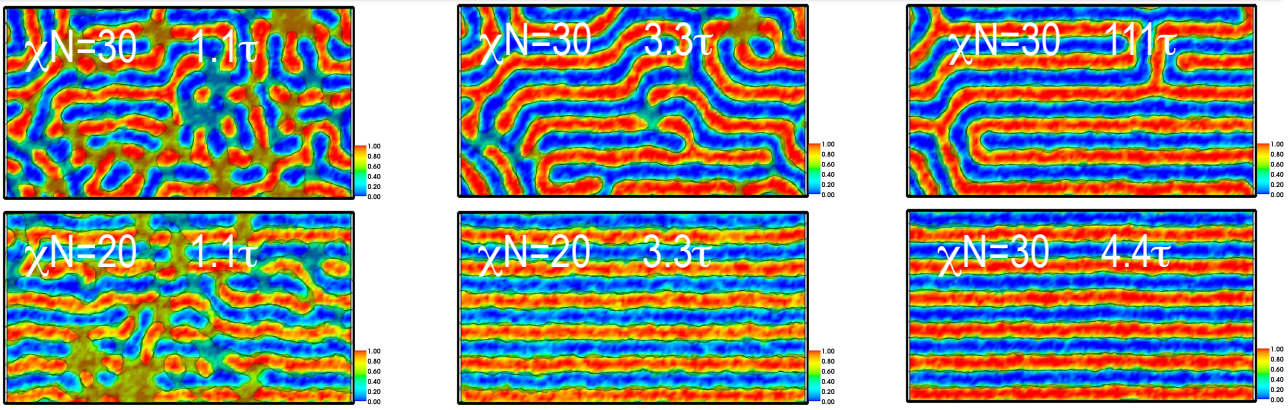

kinetics of structure formation: thin-film *versus* directed self-assembly

	thin-film self-assembly	**directed self-assembly (DSA)**
spinodal self-assembly: fingerprint pattern $\tau=R_{eo}^2/D$	spontaneous growth of (most) instable mode	guiding fields direct spinodal structure formation 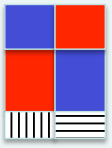
local defect annihilation and grain formation	***defects move in response to strain-field mediated interactions, defects collide and annihilate***	
late stage: grain coarsening	universal power-law behavior of grain growth, grain boundary motion	defect-free assembly already achieved because guiding fields dictate grain orientation and registration

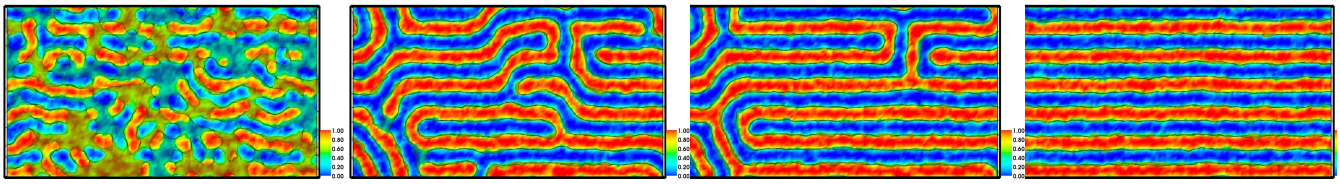

early stages: surface-directed spinodal ordering

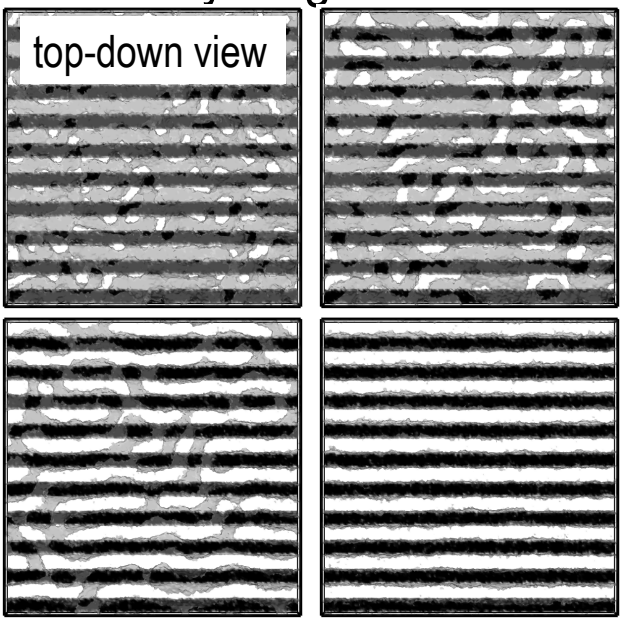

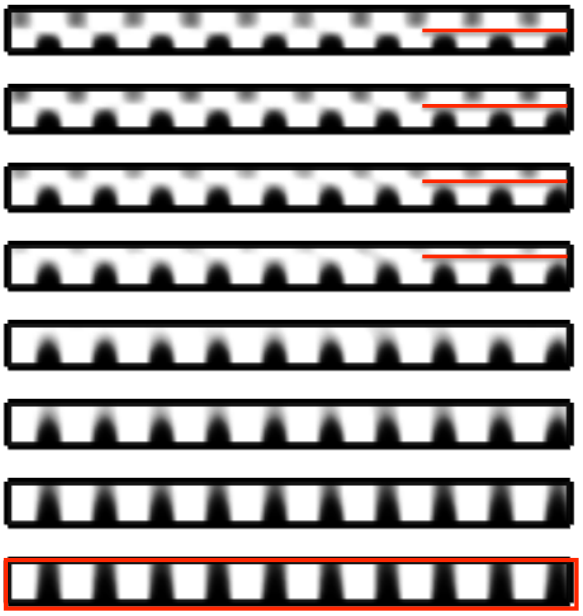

t = 1000, 3000, 8000, 14000 SMC

$\tau = R_{ee}^2/D$= 8990 SMC (≈ 1 min)

t = 1000, 2000, 3000, 4000, 5000, 6000, 8000, 10000 SMC

χN=30, 1:1 pattern replication, symmetric stripe pattern W/L_0=1/2, ΛN=±2

➡ rapid, defect-free pattern replication via formation of checkerboard pattern

Müller, Li, Orozco Rey, Welling, *J. Phys.: Conf. Ser.* **640**, 012010 (2015)

early stages: surface-directed spinodal ordering

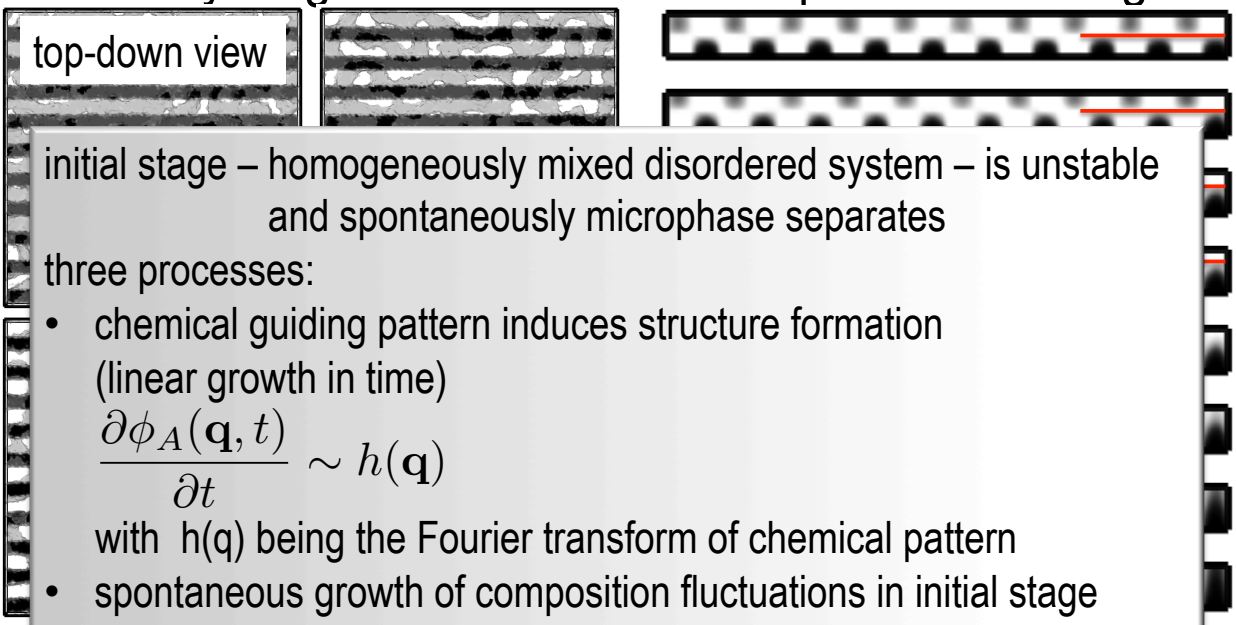

initial stage – homogeneously mixed disordered system – is unstable and spontaneously microphase separates

three processes:

- chemical guiding pattern induces structure formation (linear growth in time)

$$\frac{\partial \phi_A(\mathbf{q},t)}{\partial t} \sim h(\mathbf{q})$$

with h(q) being the Fourier transform of chemical pattern

- spontaneous growth of composition fluctuations in initial stage (exponential growth in time) ➡ checkerboard structure
- film consists of registered bottom and shifted top grain interface (grain boundary) moves to top of film

t),

χN

➡ rapid, defect-free pattern replication via formation of checkerboard pattern

Müller, Li, Orozco Rey, Welling, *J. Phys.: Conf. Ser.* **640**, 012010 (2015)

dislocation climb – no barrier for motion parallel to stripes

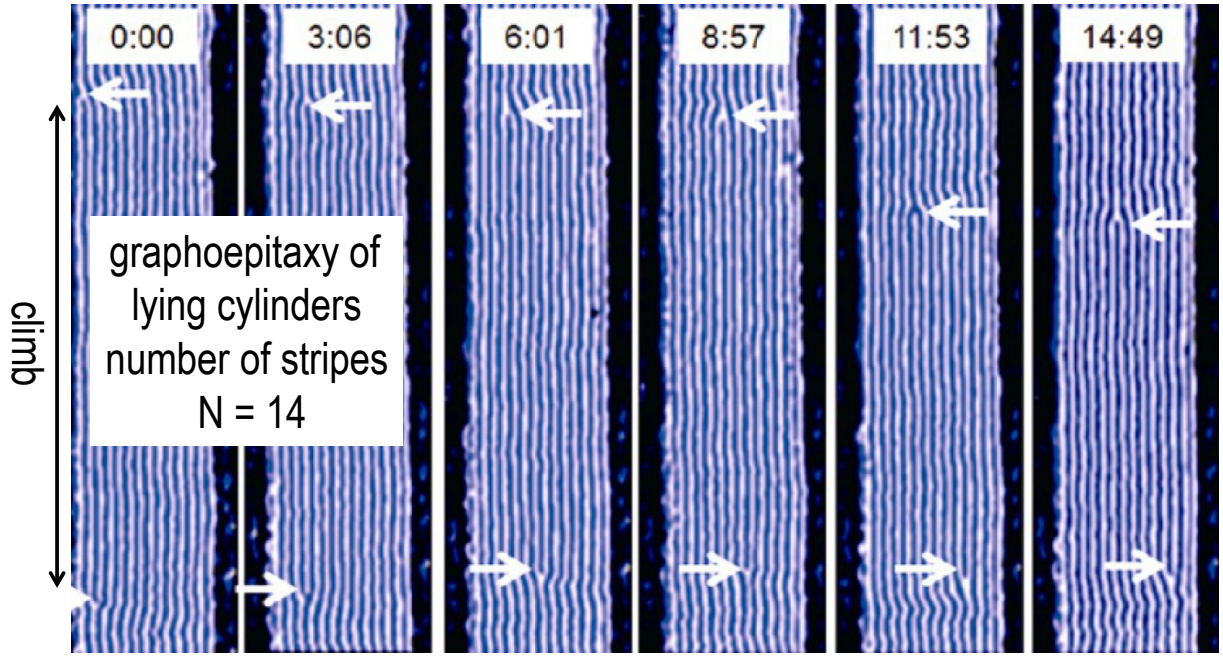

attractive force between edge dislocations with opposite Burgers vectors

Peach-Koehler force ~ -c/L, overdamped motion: velocity ~ $\nu c/L$

➡ $L^2(t)=a-Dt$ with $D=2\nu c$

Tong, Sibener, *Macromolecules* **46**, 8538 (2013)

dislocation motion – glide and climb

system: dislocation pair, χN=30, non-patterned surface
particle simulations using Single-Chain-in-Mean-Field algorithm

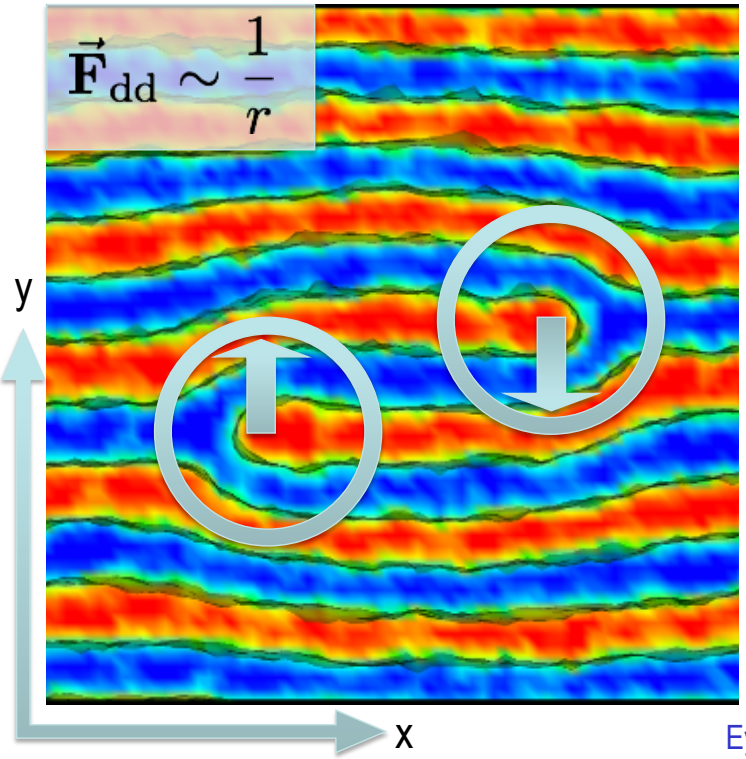

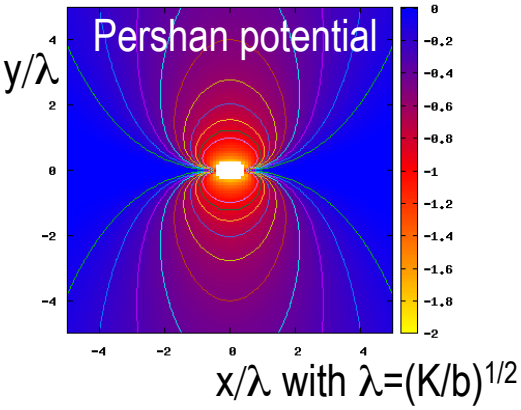

strain-field mediated attraction between edge dislocations with opposite Burgers vectors

➡ ***Peach-Koehler force***

Peach, Koehler, *Phys. Rev.* **80**, 436 (1950)
Pershan, *J. Appl. Phys.* **45**, 1590 (1974)
Eykholt, Srolovitz, *J. Appl. Phys.* **65**, 4204 (1989)

dislocation glide – barrier for motion perpendicular to stripes

system: dislocation glide by half a period, χN=30, non-patterned surface
self-consistent field theory (SCFT) calculations / string method F[W]

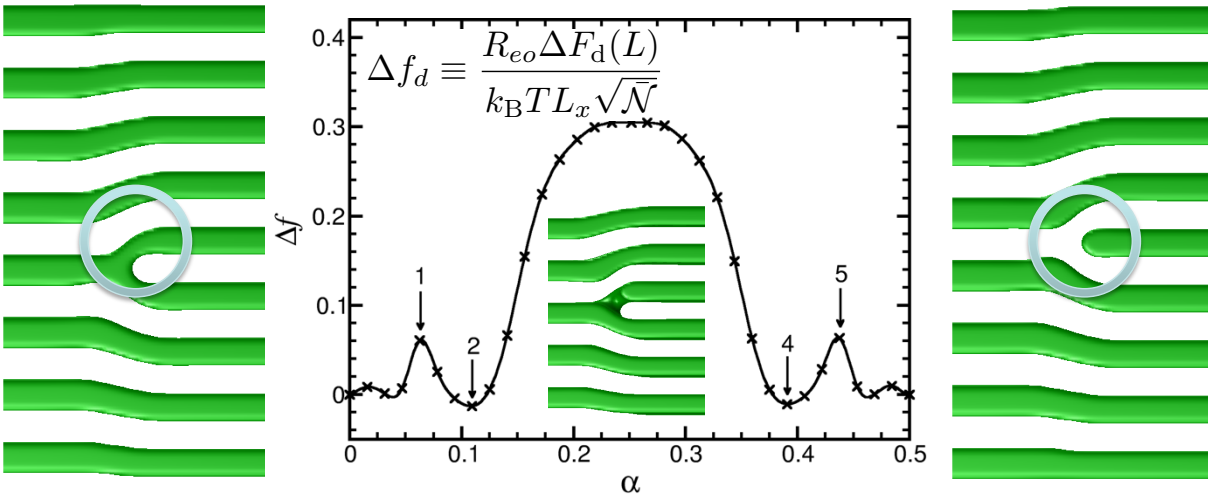

defect motion perpendicular to stripes involves domain breaking (barrier)

- very low defect mobility for perpendicular glide motion
- perpendicular distance between edge dislocations remains conserved
- translation invariance along stripes ➡ **no barrier for climb motion**

Li, Müller, *Macromolecules* **49**, 6126 (2016)

dislocation climb: which defect annihilates first?

system: dislocation pair, χN=30, no pattern, different "**impact parameters**" particle simulations using Single-Chain-in-Mean-Field algorithm

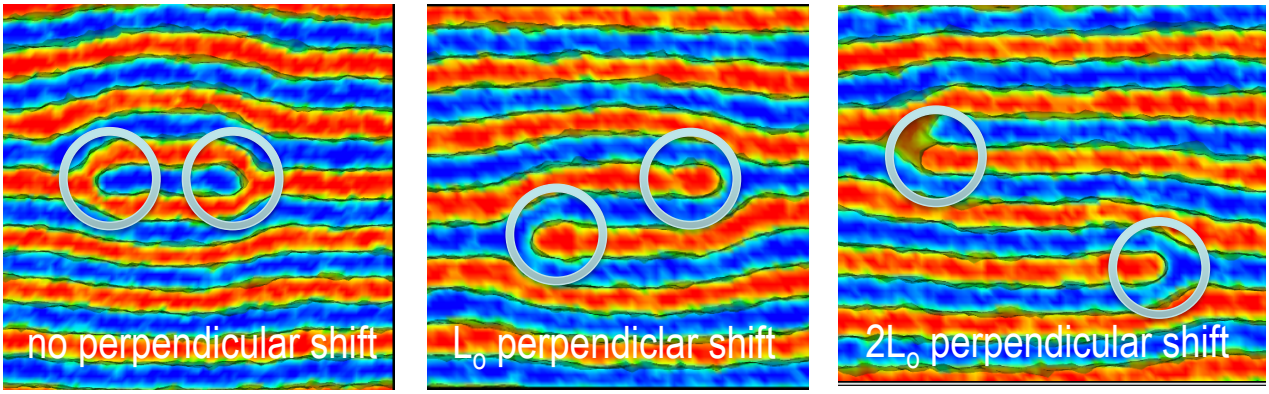

dislocation pair with opposite Burgers vectors (different perp. distances)

➡ attractive Peach-Koehler force results in defect motion parallel to stripes

questions:

a) how large is the attractive force?

b) how fast does the defect move?

c) does defect motion/collision result in defect annihilation?

dislocation climb

unconstraint climb: $1.26R_{eo} \times 22.67R_{eo} \times 10.07R_{eo}$

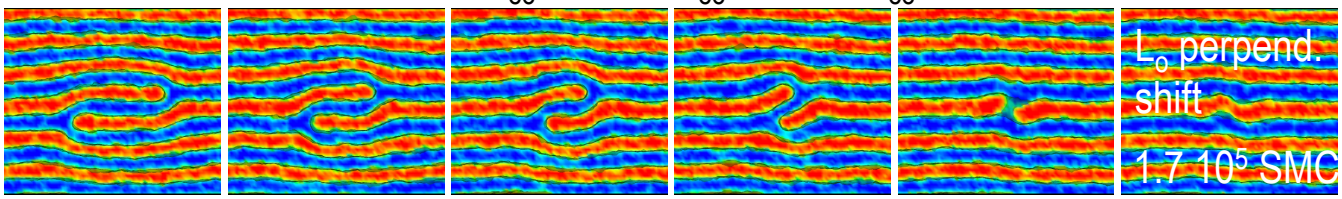

$t/\tau = 0$ 5.62 11.23 16.85 19.44 ***20***

evaporation climb: $1.26R_{eo} \times 12.5925R_{eo} \times 25.185R_{eo}$

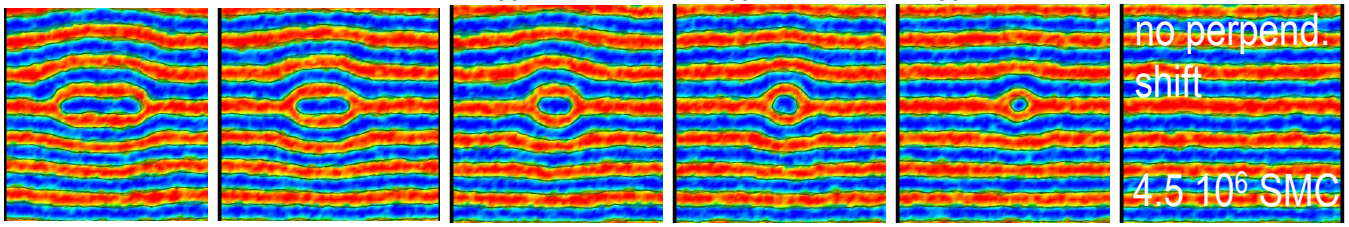

$t/\tau = 0$ 112 225 337 449 ***506***

stagnation climb – metastable dipole: $1.26R_{eo} \times 15.11R_{eo} \times 10.07R_{eo}$

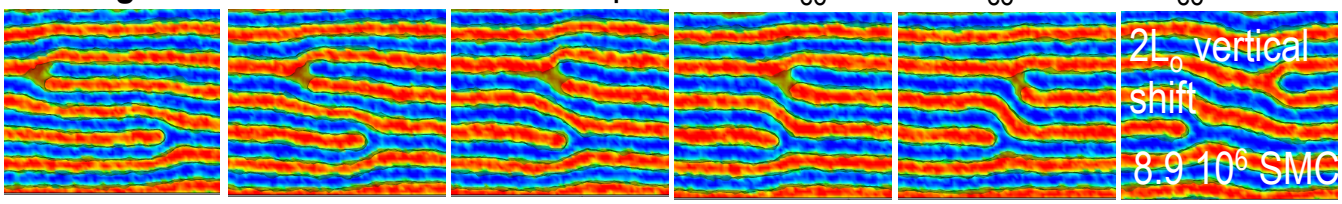

$t/\tau = 0$ 5.62 11.23 16.85 28 ***1000 …***

a) how large is the attractive force?

system: dislocation pair, χN=30, non-patterned surface
SCFT calculations, string method F[W]

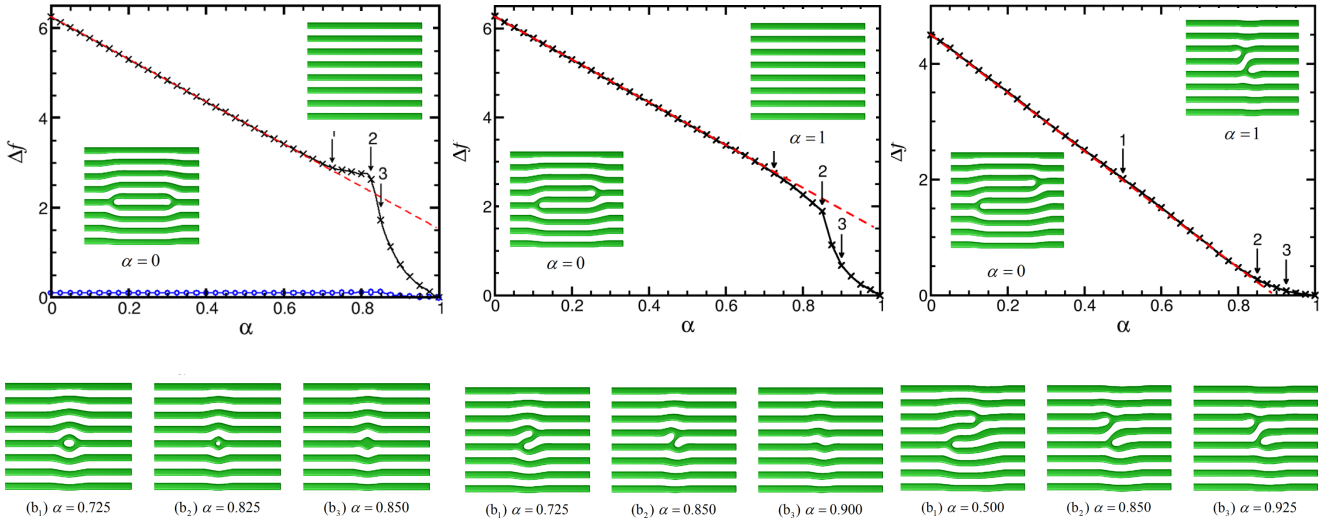

excess free energy depends linearly on distance L (parallel to stripes)
thermodynamic driving force: excess free energy of extra half lamella

$$\Delta F_{\mathrm{d}} \sim L \Rightarrow -\frac{\partial \Delta F_{\mathrm{d}}}{\partial L} = \mathrm{const}$$ and **same magnitude for all 3 cases**

Li, Müller, *Macromolecules* **49**, 6126 (2016)

a) how large is the attractive force?

system: dislocation pair, χN=30, non-patterned surface
SCFT calculations, string method F[W]

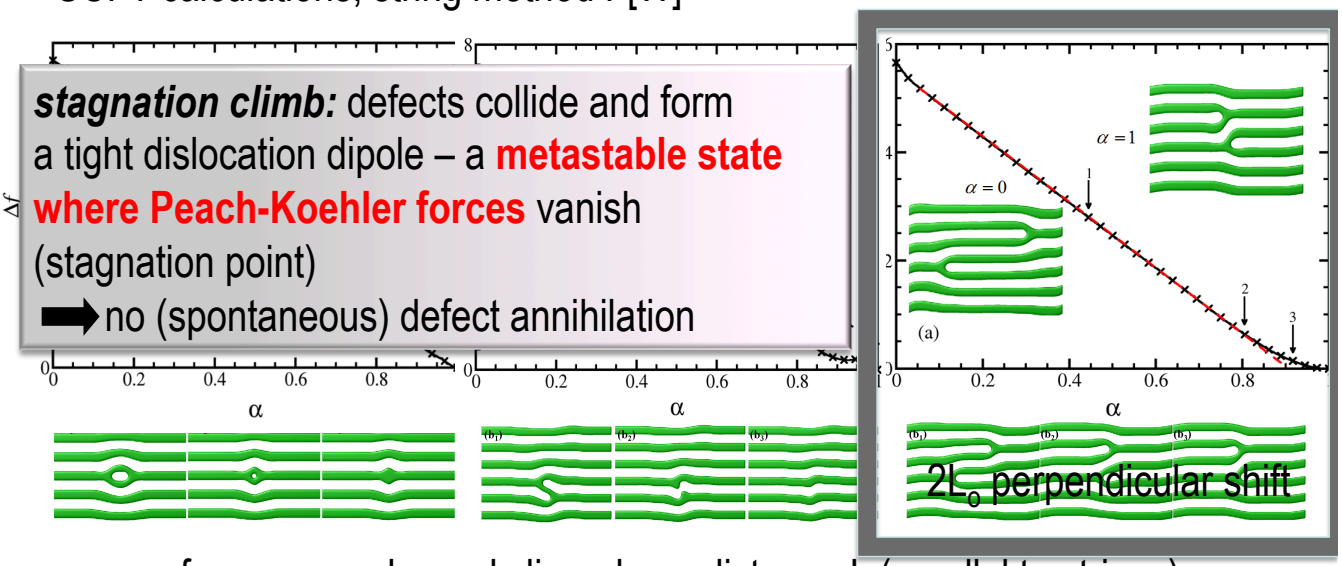

stagnation climb: defects collide and form a tight dislocation dipole – a **metastable state where Peach-Koehler forces** vanish (stagnation point)
➡ no (spontaneous) defect annihilation

excess free energy depends linearly on distance L (parallel to stripes)
thermodynamic driving force: excess free energy of extra half lamella

$$\Delta F_{\mathrm{d}} \sim L \Rightarrow -\frac{\partial \Delta F_{\mathrm{d}}}{\partial L} = \mathrm{const}$$ and **same magnitude for all 3 cases**

Li, Müller, *Macromolecules* **49**, 6126 (2016)

a) how large is the attractive force?

system: dislocation pair, χN=30, non-patterned surface, $(24L_o)^2$
SCFT calculations, L_o=1.825R_e, f=1/2

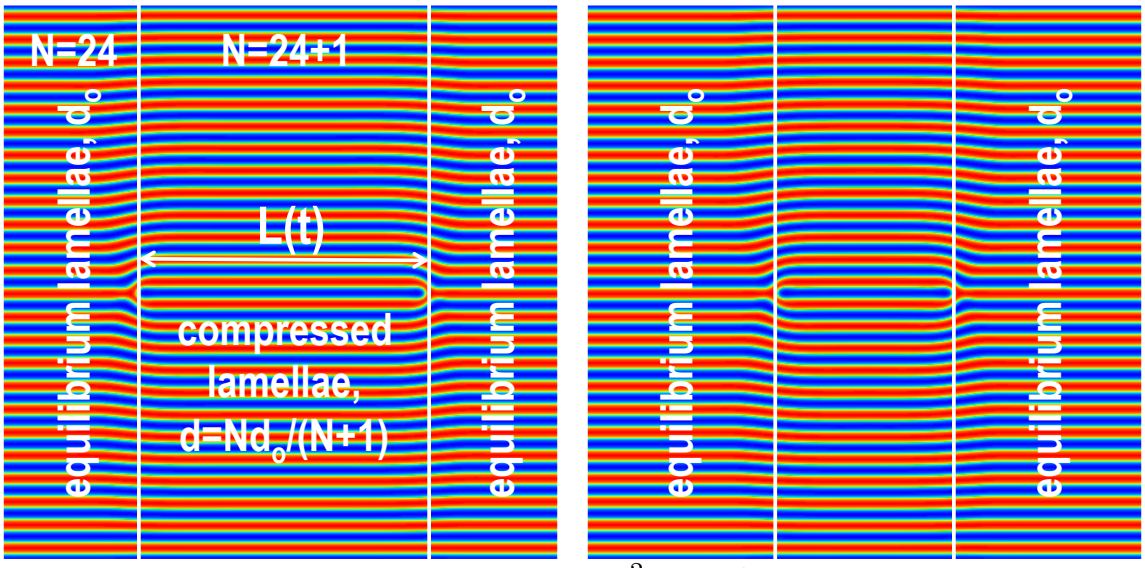

$$\Delta F_{\mathrm{d}} \sim LN(d-d_0)^2 = Ld_0^2\left(\frac{N}{N+1}-1\right)^2 \approx \frac{Ld_0^2}{N}$$

$$\Delta F_{\mathrm{d}} \sim L \Rightarrow -\frac{\partial \Delta F_{\mathrm{d}}}{\partial L} = \mathrm{const}$$

Li, Müller, *Macromolecules* **49**, 6126 (2016)

a) how large is the attractive force?

system: dislocation pair, χN=30, non-patterned surface, $(24L_o)^2$
SCFT calculations, L_o=1.825R_e, f=1/2

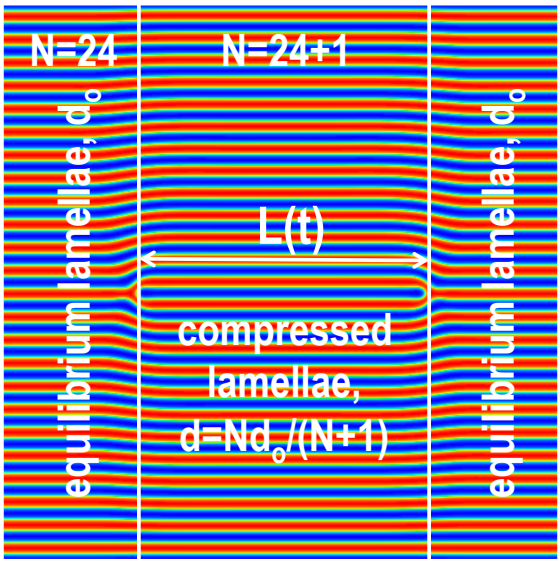

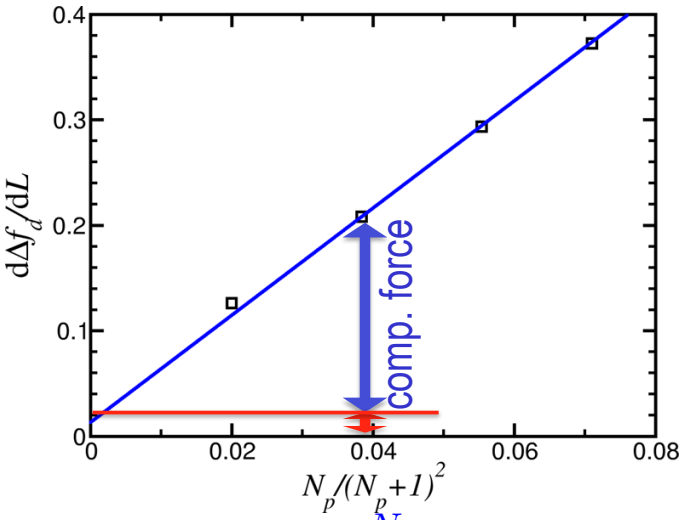

$$\Delta f_d = c_1 L \frac{N}{(N+1)^2} + c_2 \ln L + c_3$$

$$\frac{d\Delta f_d}{dL} = c_1 \frac{N}{(N+1)^2} + c_2 \frac{1}{L}$$

$$\Delta F_{\mathrm{d}} \sim L \Rightarrow -\frac{\partial \Delta F_{\mathrm{d}}}{\partial L} = \mathrm{const}$$

➡ compression force dominates over PK force due to finite-size effects

a) how large is the attractive force?

system: dislocation pair, $\chi N=30$, non-patterned surface
SCFT calculations, $L_o=1.825R_e$, f=1/2

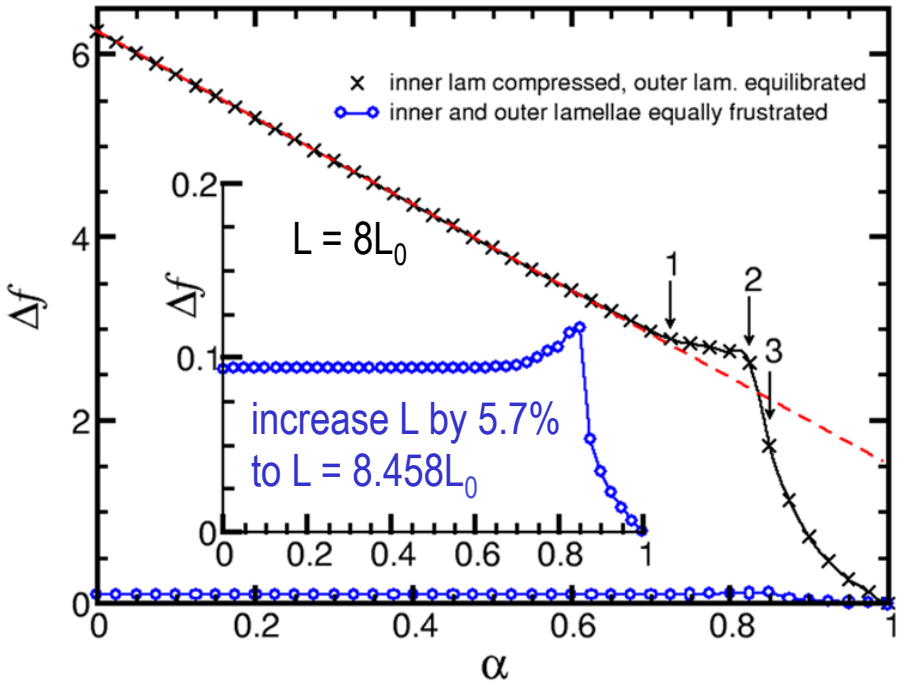

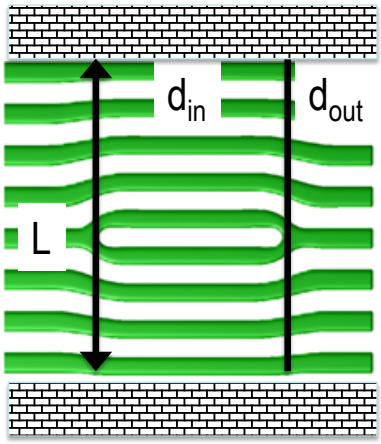

a) $d_{out}=L_0$, $d_{in}<L_0$
$f(d_{out})<f(d_{in})$

b) $d_{out}>L_0$, $d_{in}<L_0$
so that $f(d_{out})=f(d_{in})$

⇒ no compression force
PK very weak
barrier for annihilation

compression force also dictates dislocation glide

system: dislocation glide by half a period, χN=30, non-patterned surface self-consistent field theory (SCFT) calculations / string method F[W]

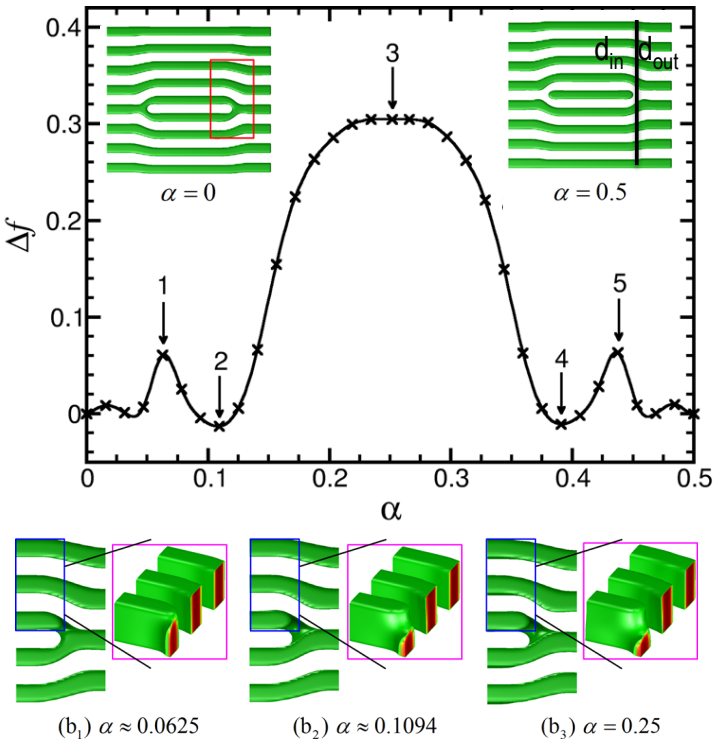

- states 2 and 4 correspond to metastable half-broken domains

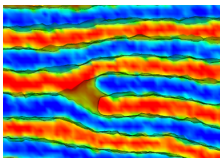

- main barrier of glide arises from subtle shift of domains by $\Delta y \sim 1/L_y$

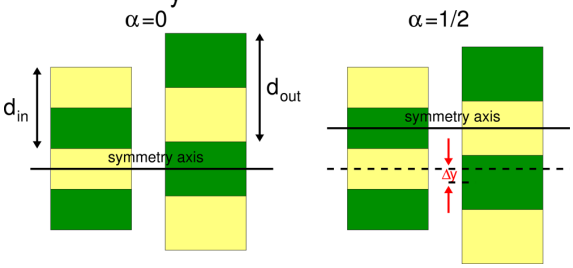

Li, Müller, *Macromolecules* **49**, 6126 (2016)

b) how fast does defect move: unconstraint vs evaporation

system: dislocation pair, χN=30, non-patterned surface
particle simulations using Single-Chain-in-Mean-Field algorithm

evaporation climb

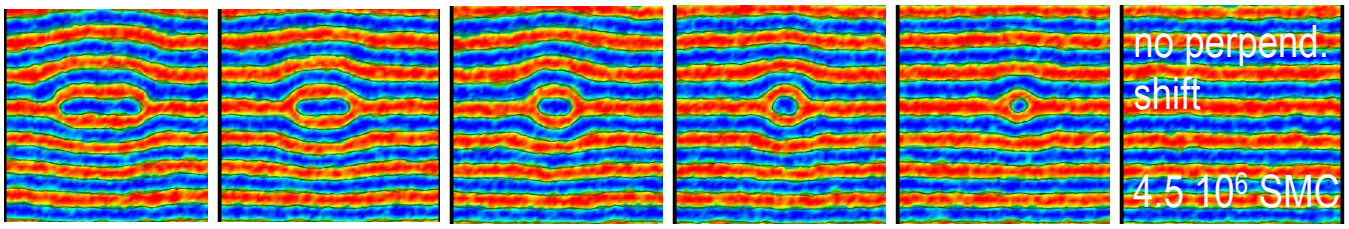

t/τ = 0 | 112 | 225 | 337 | 449 | ***506***

unconstraint climb

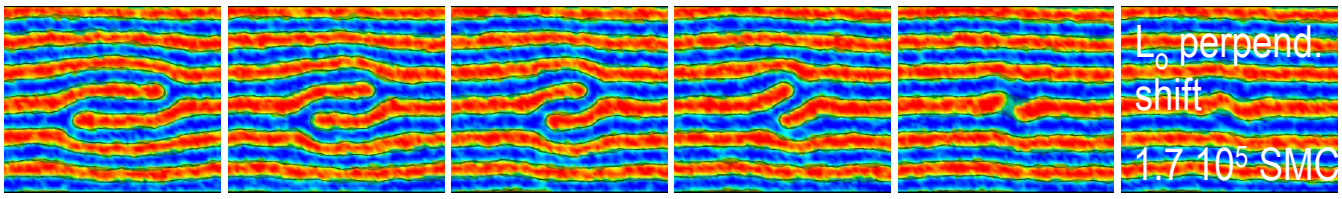

t/τ = 0 | 5.62 | 11.23 | 16.85 | 19.44 | ***20***

➡ both climbs remove defect, but evaporation climb is qualitatively slower

b) how fast does defect move: unconstraint vs evaporation

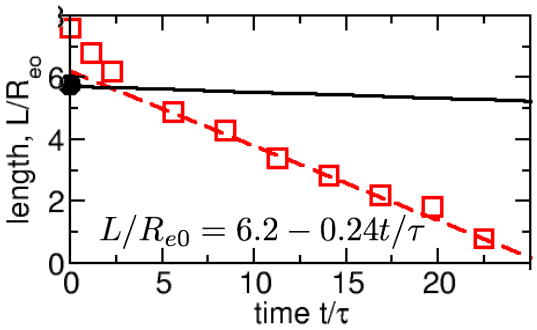

unconstraint climb:
viscous response to force

$$\frac{\mathrm{d}L}{\mathrm{d}t} \sim -\frac{\partial \Delta F_\mathrm{d}}{\partial L}$$

➡ constant velocity,
linear decrease of L

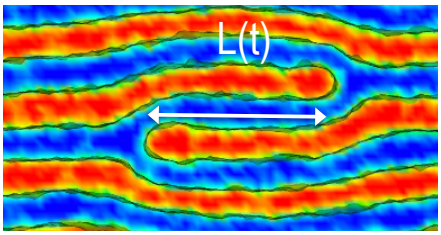

Li, Müller, *Macromolecules* **49**, 6126 (2016)

b) how fast does defect move: unconstraint vs evaporation

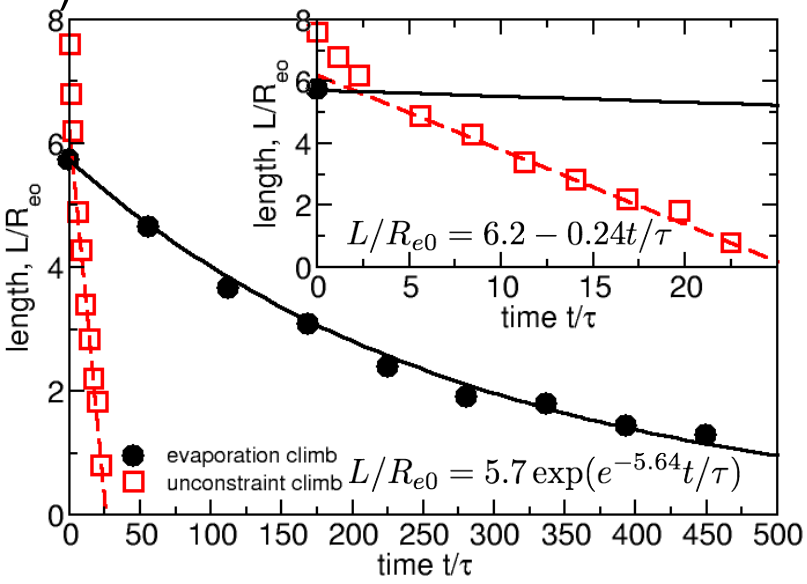

unconstraint climb:
viscous response to force

$$\frac{\mathrm{d}L}{\mathrm{d}t} \sim -\frac{\partial \Delta F_\mathrm{d}}{\partial L}$$

➡ constant velocity, linear decrease of L

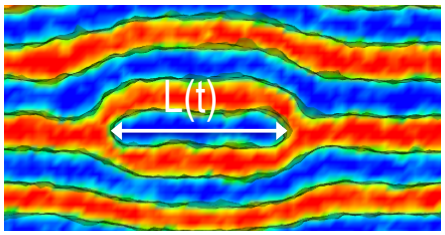

evaporation climb: constant evaporation rate, *r*, of block from extra lamella

➡ $\frac{\partial \Delta N}{\partial t} \sim -\Delta N \Rightarrow \Delta N \sim L \sim e^{-rt}$ exponential decrease of L

microscopic: blue blocks in extra half lamella "**evaporate**", single blocks diffuse through red domain and must overcome free energy barrier ~ $\chi N f k_B T$

macroscopic: $\nabla\mu$ aims at shrinking L, but does not efficiently translate into current, small $\Lambda \sim D\phi_A\phi_B \sim e^{-f\chi N}$ Müller, Daoulas, *Phys. Rev. Lett* **107**, 227801 (2011)

c) does defect motion/collision result in defect annihilation?

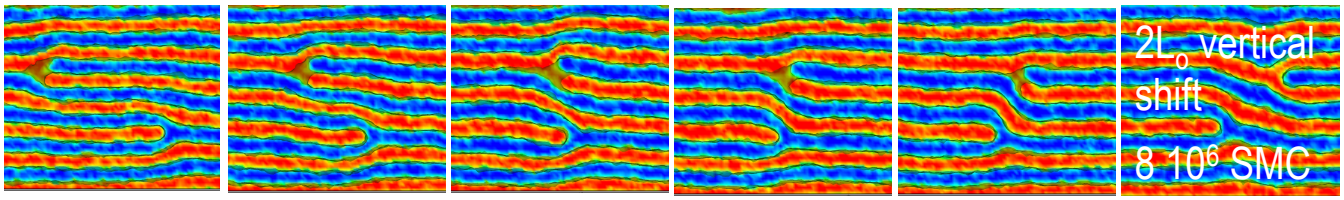

t/τ = 0 5.62 11.23 16.85 28 ***899***

stagnation climb: motion arrests in a metastable configuration
here: tight dislocation dipole

defect annihilation is a thermally activated process

➡ **protracted annihilation time** because $\Delta F_{\mathrm{d}} \sim \Delta F_{\mathrm{b}} \sim k_{\mathrm{B}} T \sqrt{\bar{\mathcal{N}}}$

questions:

a) what is the microscopic mechanism of defect annihilation?

b) what are the concomitant activation free energies (barriers)?

➡ study ***Minimum Free-Energy Path (MFEP)*** by string method

Li, Nealey, de Pablo, Müller, *Phys. Rev. Lett.* **113**, 168301 (2014)

on-the-fly string method and improved string method

describe transformation path by a string of morphologies $m_s(\mathbf{r})$ with contour variable $0 \le s \le 1$

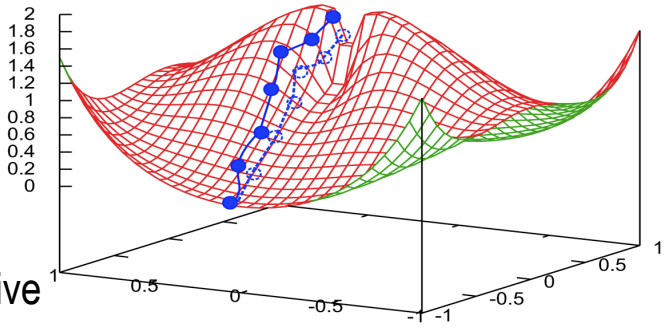

minimum free-energy path (MFEP) is defined by condition that the derivative perpendicular to the path vanishes

improved string method: E, Ren, Vanden-Eijnden, *J. Chem. Phys.* **126**, 164103 (2007)

1. evolve each morphology $m_s(\mathbf{r})$ as to minimize the free energy

$$\frac{\delta F_c[m_c]}{\delta m_c(\mathbf{r})} = \lambda k_B T \left[m_c(\mathbf{r}) - \langle \hat{m}(\mathbf{r}) \rangle_c\right] \overset{\lambda \to \infty}{\to} \mu(\mathbf{r}|m_c) \qquad \Delta m_s(\mathbf{r}) = -\mu(\mathbf{r}|m_s)\Delta$$

2. re-parameterize the string to equal distance Δs (pointwise 3rd order spline)

SCFT: Cheng, Lin, E, Zhang, Shi, *Phys. Rev. Lett.* **104**, 148301 (2010); Ting, Appelö, Wang, *Phys. Rev. Lett.* **106**, 168101 (2011); Li, Nealey, de Pablo, Müller, *Phys. Rev. Lett.* **113**, 168301 (2014)

particle simulations: Maragliano, Vanden-Eijnden. *Chem. Phys. Lett.*, **446**, 182 (2007); Miller, Vanden-Eijnden, Chandler, *PNAS* **104**, 14559 (2007); Müller, Smirnova, Marelli, Fuhrmans, Shi, *Phys. Rev. Lett.* **108**, 228103 (2012); Müller, Sun, *Phys. Rev. Lett.* **111**, 267801 (2013); Hur, Thapar, Ramirez-Hernandez, Khaira, Segal-Peretz, Rincon-Delgadillo, Li, Müller, Nealey, de Pablo, *PNAS* **112**, 14144 (2015)

interface models: Giacomello, Meloni, Müller, Casciola, *J. Chem. Phys.* **142**, 104701 (2015), Ryham, Klotz, Yao, Cohen, *Biophys. J.* **110**, 1110 (2016)

defect annihilation by ***lateral*** interface motion (2D)

system: dislocation pair

Minimum Free-Ener … SCFT theory

2D mechanism (3D …

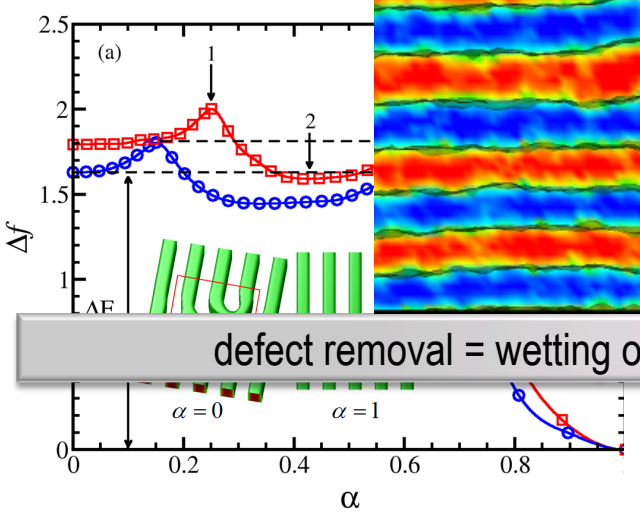

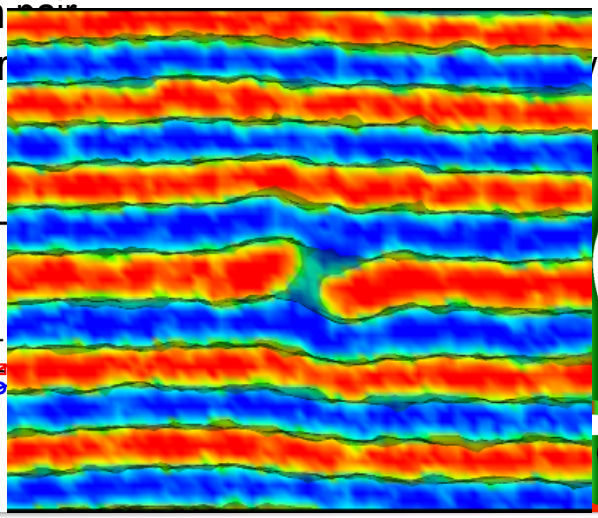

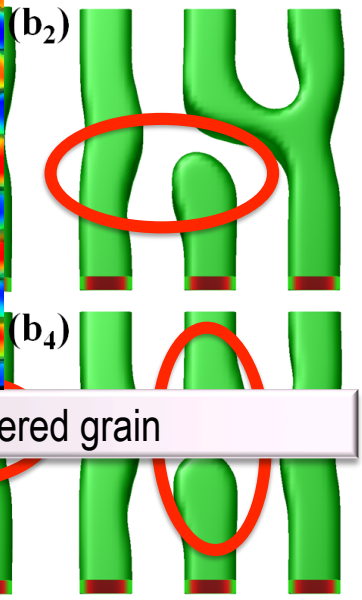

defect removal = wetting of the aligned, registered grain

without guiding pattern, ΛN=0

sequential breaking of connections

2D calculation for graphoepitaxy see Takahashi, *et al, Macromolecules* **45**, 6253 (2012)

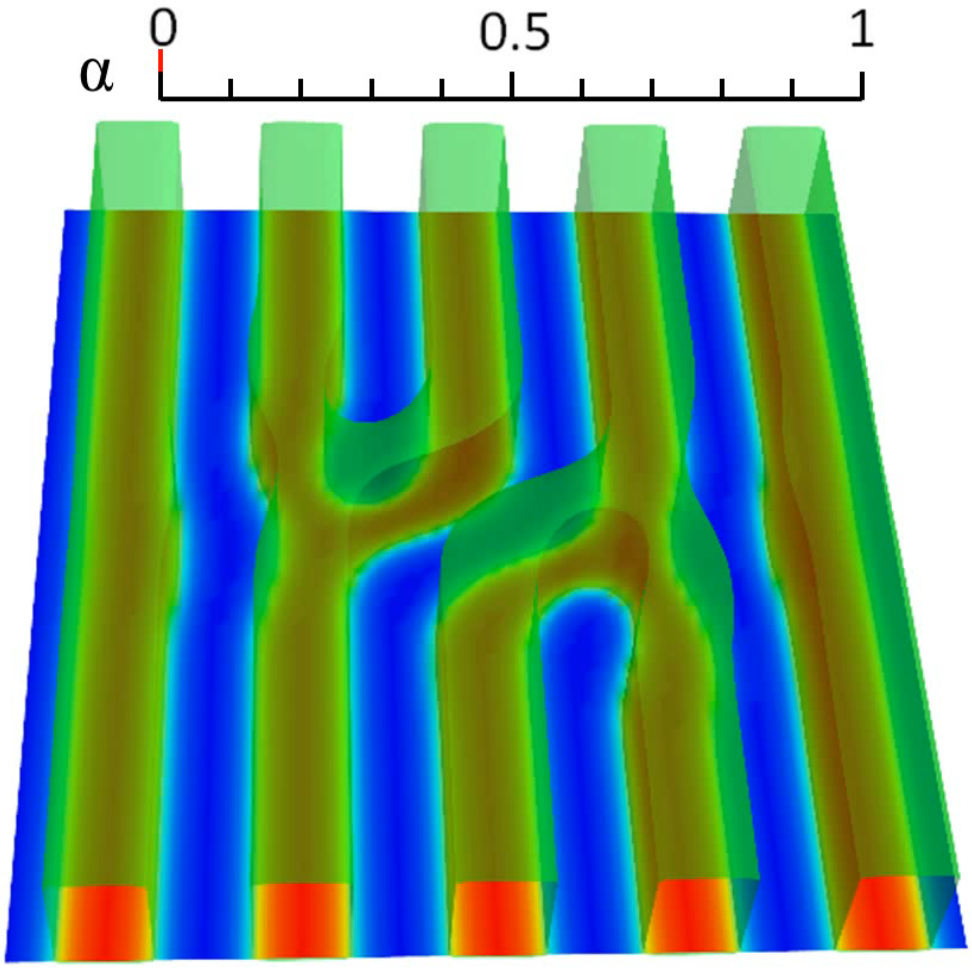
α
0
0.5
1

defect annihilation by ***perpendicular*** interface motion

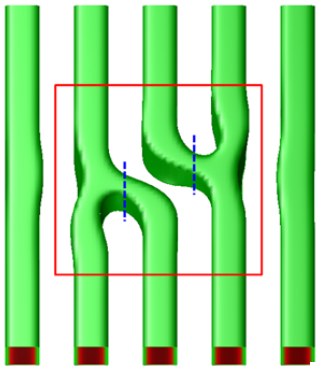

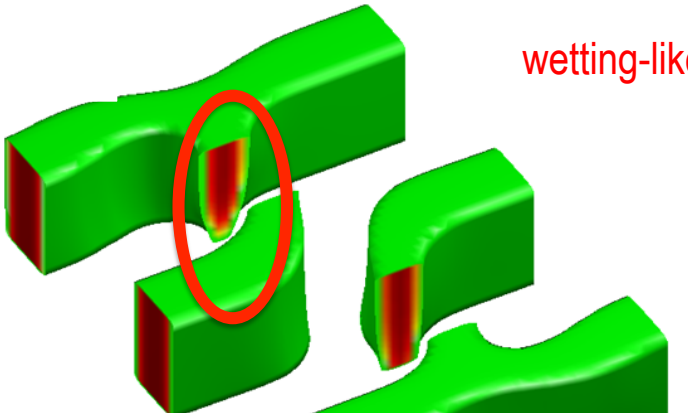

wetting-like mechanism

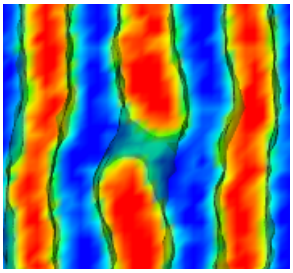

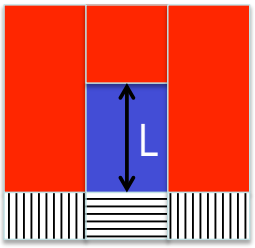

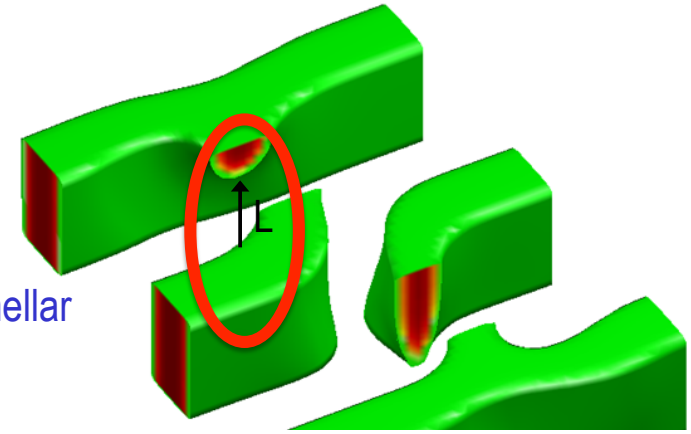

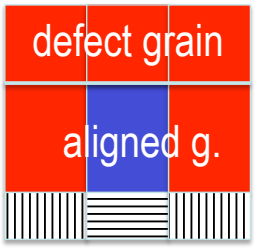

wetting of half lamellar domain on stripe

wetting of aligned grain on patterned substrate

Li, Nealey, de Pablo, Müller, *Phys. Rev. Lett.* **113**, 168301 (2014)

defect annihilation by ***perpendicular*** interface motion

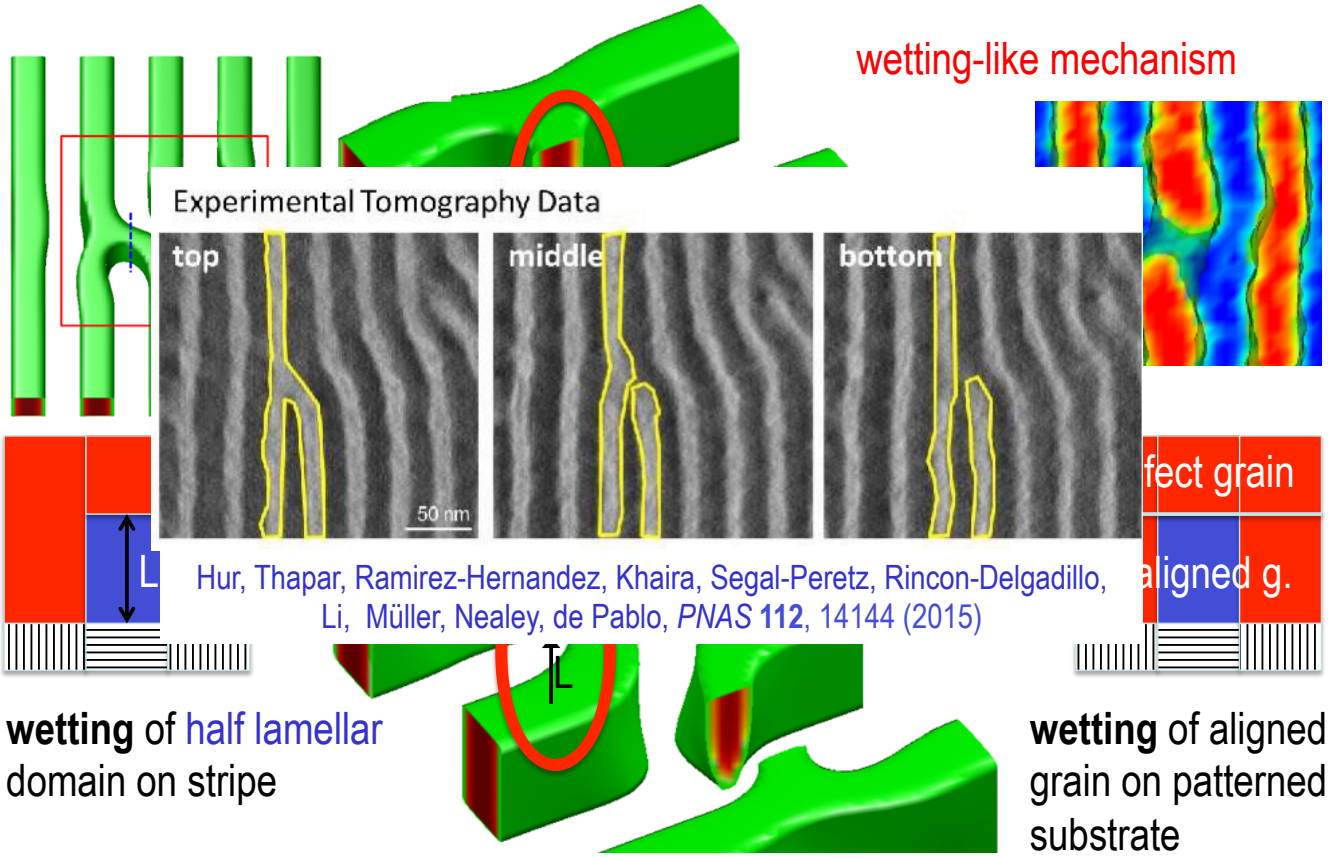

Hur, Thapar, Ramirez-Hernandez, Khaira, Segal-Peretz, Rincon-Delgadillo, Li, Müller, Nealey, de Pablo, *PNAS* **112**, 14144 (2015)

wetting of half lamellar domain on stripe

wetting of aligned grain on patterned substrate

Li, Nealey, de Pablo, Müller, *Phys. Rev. Lett.* **113**, 168301 (2014)

defect annihilation by ***perpendicular*** interface motion

system: dislocation pair

Minimum Free-Energy Path (MFEP) of F[W] obtained by SCFT theory

wetting-like mechanism

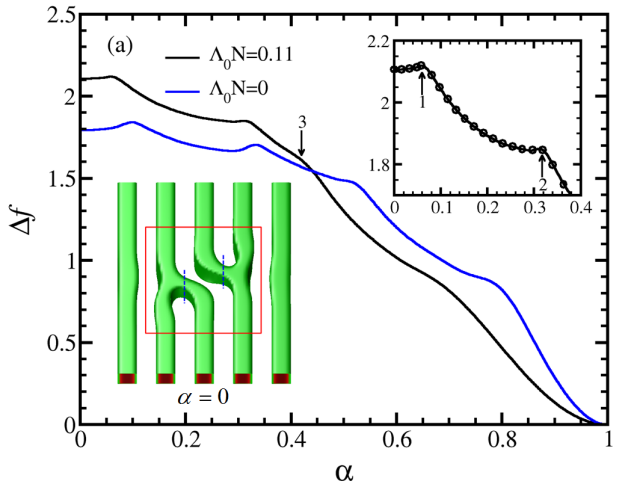

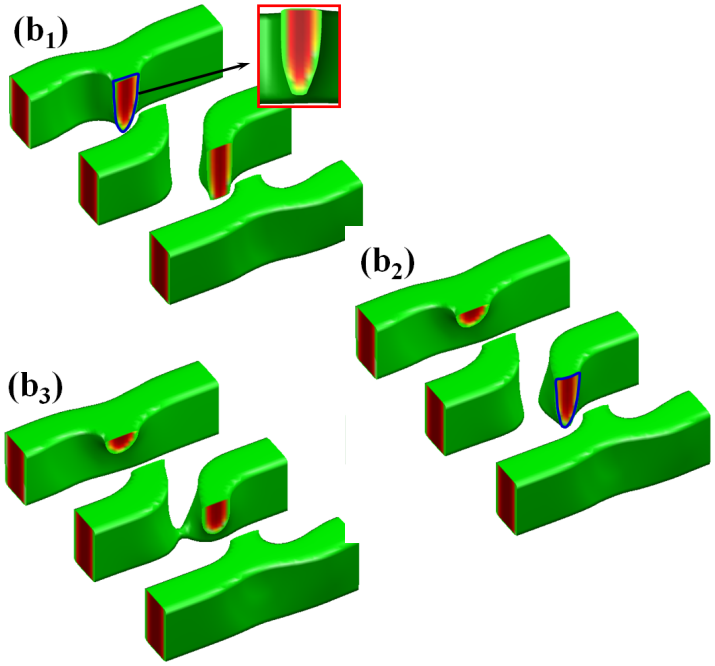

without and with guiding pattern

sequential breaking of connections

Li, Nealey, de Pablo, Müller, *Phys. Rev. Lett.* **113**, 168301 (2014)

defect annihilation for larger “impact parameter”

system: dislocation pair, χN=20, 3×density multiplication, 3 L_0 perp. shift
Minimum Free-Energy Path (MFEP) obtained by particle simulation

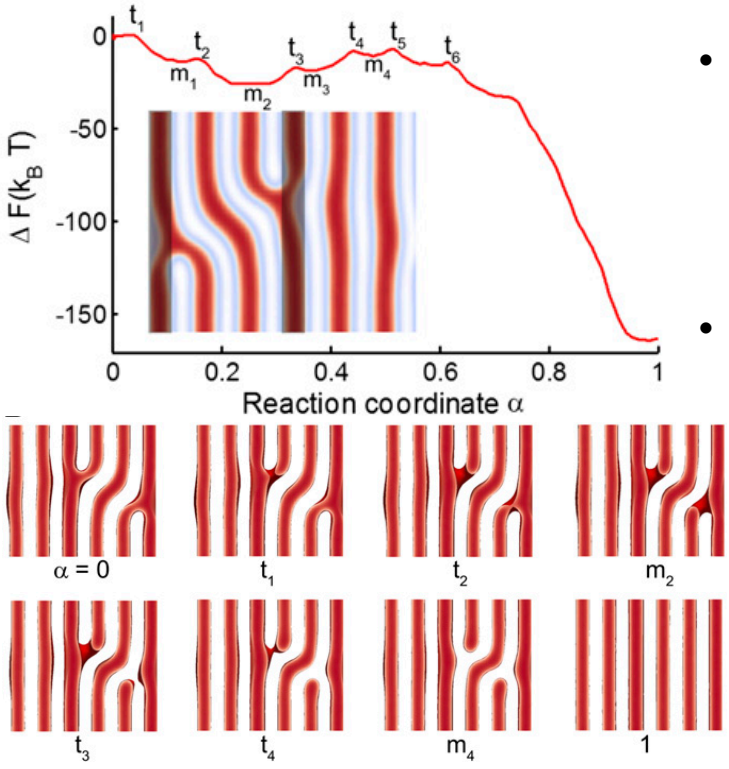

- defect annihilation involves dislocation glide and breaking of connections via a wetting-like mechanism
  ➡ multiple barriers
- pathway and barrier depends on relative position of defects cores with respect to guiding pattern

Hur, Thapar, Ramírez-Hernández, Khaira, Segal-Peretz, Rincon-Delgadillo, Li, Müller, Nealey, de Pablo, *PNAS* **112** 14144 (2015)

defect removal is enhanced close to ODT

system: dislocation pair

Minimum Free-Energy Path (MFEP) of F[W] obtained by SCFT theory

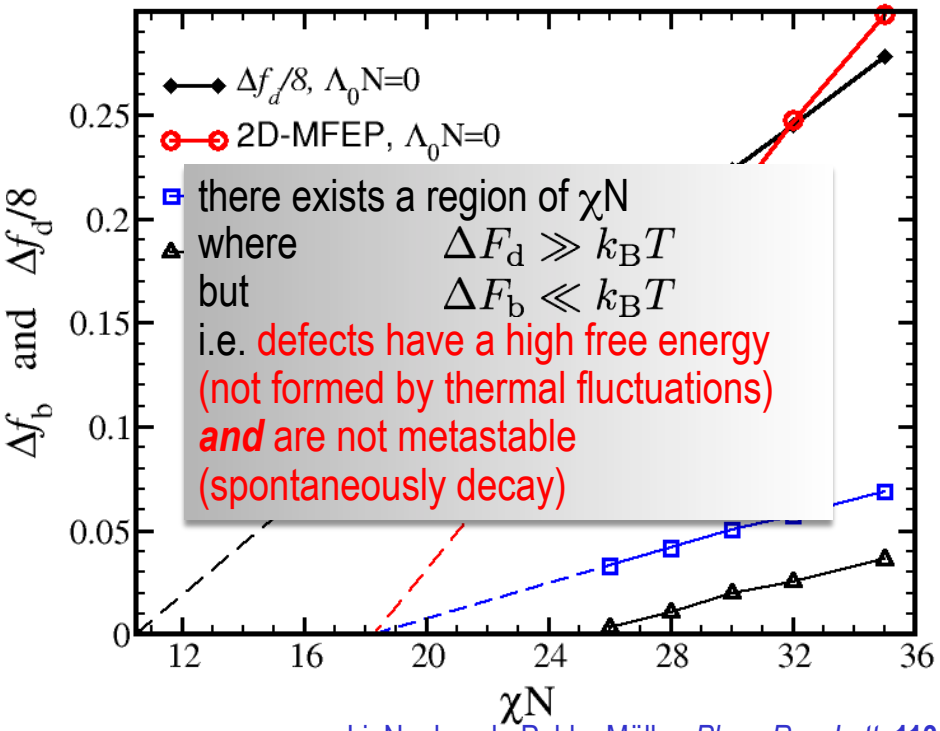

there exists a region of χN

where $\Delta F_{\mathrm{d}} \gg k_{\mathrm{B}}T$

but $\Delta F_{\mathrm{b}} \ll k_{\mathrm{B}}T$

i.e. defects have a high free energy (not formed by thermal fluctuations) ***and*** are not metastable (spontaneously decay)

Li, Nealey, de Pablo, Müller, *Phys. Rev. Lett.* **113**, 168301 (2014)

process-directed self-assembly: defect removal at low χN

system: dislocation pair
particle simulations using Single-Chain-in-Mean-Field algorithm
stagnation climb – metastable dipole

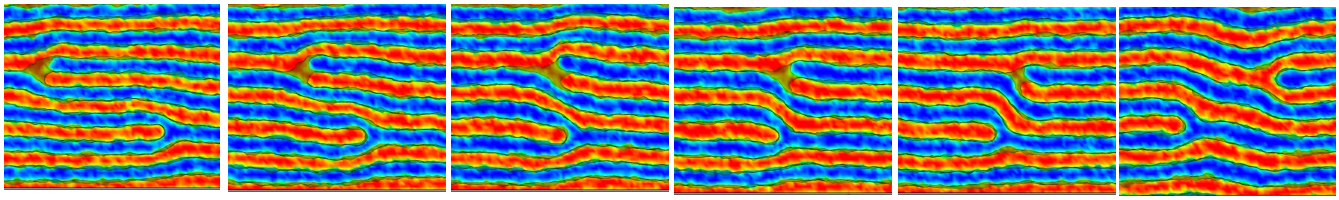

t/τ = 0 5.62 11.23 16.85 28 **1000**

observation at χN=30: distance between dislocations decreases in time
collide and form a metastable tight dislocation dipole

quench from χN=30 to 20 renders tight dislocation dipole unstable

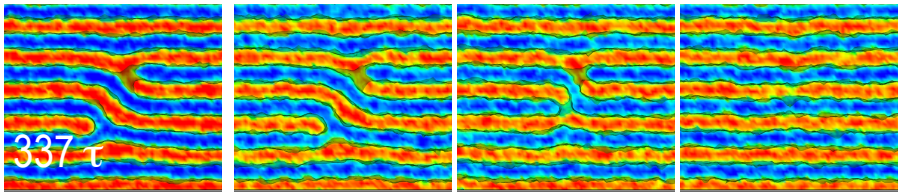

t/τ = 0 0.11 4.5 ***5.4***

process-directed self-assembly: defect removal at low χN

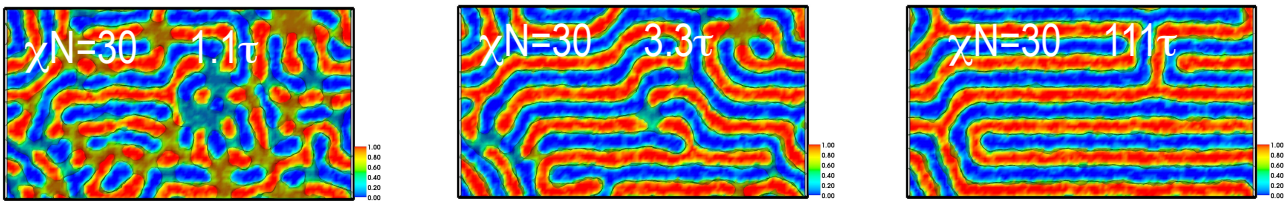

L/S pattern – no density multiplication
eliminate well-formed metastable disclinationdefects (111τ@χN=30)
by reducing χN=30➔20

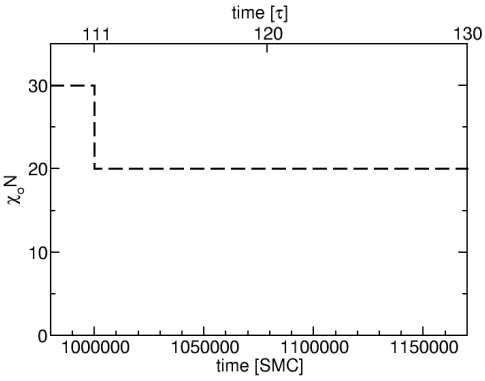

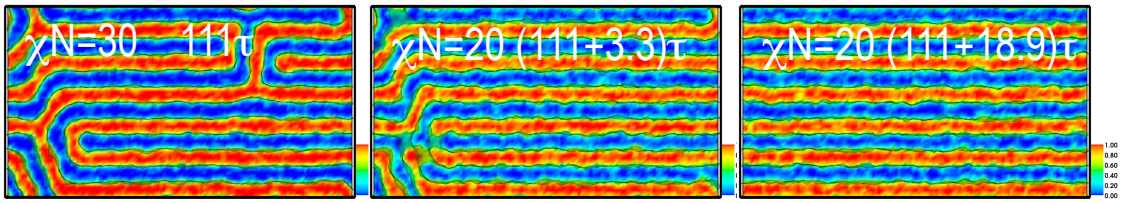

➡ defect are eliminated
but time scale is longer than ordering from disordered state at χN=20

summary

- excess free-energy of defects is prohibitive $\Delta F \sim O(100 k_B T)$:
  defects will not spontaneously form but arise in course of structure formation
- local smectic-A geometry controls defect motion and collision
  deviation from Peach-Koehler force due to boundary/finite-size effects
- **defect removal fast at intermediate segregations, $\chi N_* \approx 18$**
  process window increases with preference of guiding pattern

process-directed self-assembly: tailor free energy landscape of self-assembly by temporal control of thermodynamic state variable, e.g., χN or solvent

W.H. Li, U. Welling, J.C. Orozco Rey, S.M. Hur, P.F. Nealey, J.J. de Pablo